View Article Online
View Journal

Dalton Transactions

An international journal of inorganic chemistry

Accepted Manuscript

This article can be cited before page numbers have been issued, to do this please use: X. Lin, Y. Zhao, S. Qiao, Z. Sun, O. Santoro and C. Redshaw, *Dalton Trans.*, 2020, DOI: 10.1039/C9DT04332B.

ROYAL SOCIETY OF CHEMISTRY

rsc.li/dalton

View Article Online
DOI: 10.1039/C9DT04332B

Synthesis and structures of mono- and di-nuclear aluminium and zinc complexes bearing α-diimine and related ligands, and their use in the ring opening polymerization of cyclic esters

Lin Xiao,[a] Yanxia Zhao,[a*] Sijie Qiao,[a] Ziyue Sun,[a] Orlando Santoro[b] and Carl Redshaw[a,b*]

[a] *College of Chemistry and Material Science, Northwest University, 710069 Xi'an, China*
[b] *Department of Chemistry & Biochemistry, The University of Hull, Cottingham Rd, Hull, HU6 7RX, U.K.*

Abstract: A series of organoaluminium imino-amido complexes of the type {[ArNC(Me$_2$)C(Me)=NAr]AlMe$_2$} (Ar = 2,6-*i*Pr$_2$C$_6$H$_3$ (**1**), Ar = 2,6-Et$_2$C$_6$H$_3$ (**2**); Ar = 2,6-Me$_2$C$_6$H$_3$ (**3**) have been prepared via reaction of AlR$_3$ and the respective α-diimine. Similar reaction of the bis(α-diimine) [ArN=C(Me)C(Me)=N-]$_2$ (Ar = 2,6-*i*Pr$_2$C$_6$H$_3$) with AlMe$_3$ afforded the bimetallic complex [ArN–C(Me)$_2$C(Me)=NAlMe$_2$]$_2$ (**4**), whilst reaction of the acetyl-imino compound [O=C(Me)C(Me)=NAr] (Ar = 2,6-Et$_2$C$_6$H$_3$) with AlMe$_3$ afforded the bimetallic complex {[OCMe$_2$CH(Me)=NAr]AlMe$_2$}$_2$ (**5**). In related organozinc chemistry, we have isolated {[ArNC(Me)(Et)C(Me)=NAr]ZnEt} (Ar = 2,6-*i*Pr$_2$C$_6$H$_3$, **6**) and the trinuclear complex {[ArN=C(Me)COCHCO(Me)C(Me)=NAr][OCH(Me)C(Me)=NAr](ZnEt)$_3$} (Ar = 2,6-*i*Pr$_2$C$_6$H$_3$, **7**) from reactions of ZnEt$_2$ with ArN=C(Me)C(Me)=NAr or [O=C(Me)C(Me)=NAr], respectively. Reaction of the bis(α-diimine), **L**$^{i\text{Pr-N}_2\text{-ArCH}_2\text{Ar-N}_2}$, derived from 4,4$^{/}$-methylenebis(2,6-diisopropylaniline), with ZnCl$_2$ affords [**L**$^{i\text{Pr-N}_2\text{-ArCH}_2\text{Ar-N}_2}$(ZnCl$_2$)$_2$] (**8**). The molecular structures of complexes **1**–**8** are reported. Preliminary results of the ability of **1**–**8**, along with the previously reported metal–metal bonded complex {[ArN=C(Me)C(Me)=NAr]Al(THF)}$_2$ (**9**), to act as catalysts for the ring opening polymerization (ROP) of the cyclic esters ε-caprolactone (ε-Cl), δ-valerolactone (δ-VL) and *rac*-lactide (*r*-LA) are presented. For ε-CL and δ-VL, best results were obtained using the metal–metal bonded complex **9**. For *r*-LA, the Al-based systems exhibited moderate activity affording only liquid oligomers, whilst the Zn-based systems performed better affording at 80 ^{o}C isotactic PLA with M_n *ca*. 10 KDa with conversions of up to 66%. The co-polymerization of ε-CL with δ-VL was also examined, and differing preferences were noted for monomer

View Article Online
DOI: 10.1039/C9DT04332B

incorporation.

Introduction

The global issues associated with the use of single use plastics and their impact on the environment have stimulated further interest in the development of more environmentally friendly polymers. One possible route for accessing such materials is via the use of ring opening polymerization (ROP) of cyclic esters using metal-based catalysts. [1] The main advantages of this route is that by manipulating the coordination environment at the metal, it is possible to control both the catalytic activity of the system and the properties of the resultant products. The choice of metal centre is dictated by a number of factors including cost, abundance, toxicity and performance. Given this, catalysts employing the metals aluminium and zinc continue to attract much attention; main group metal-based ROP systems have been recently reviewed. [2] The use of chelating ligands in many areas of polymerization catalysis has proved beneficial both in terms of catalyst stability and as an aid in the crystallization of the metal species involved. In particular, this has proved highly successful in olefin polymerization, where the use of the *N*,*N*-bi-dentate α-diimines has opened up new avenues in nickel-based catalysis. [3] Furthermore, such α-diimines are known to react with dialkylzinc or trialkylaluminium reagents under reflux, which results in the transfer of an alkyl group to the imine backbone. [4] The resulting imino-amide and pyridyl-amide complexes offer the opportunity of further investigations of possible cooperative effects.

There is also much interest in frameworks capable of binding simultaneously multiple metal centers, which stems from the possibility of utilizing beneficial cooperative effects. [5] Following on from the early nickel work, numerous frameworks capable of binding simultaneously multiple metal centers have been designed using simple condensation chemistry, for example in nickel-based chemistry, those shown in Chart S1 (see ESI) have been reported. [6] Given this extensive use of imine-based ligation in α-olefin oligo-/polymerization, we were somewhat surprised at the rather limited use of such ligation for the metal-catalyzed ROP of cyclic esters. [7] In particular, systems have been reported bearing bipyridyl or phenanroline, guanidine-pyridine, β-diiminate and more recently a number of α-diimines and amidates, as shown in chart 1 (zinc) and chart 2 (aluminium). In the case of the amidinate aluminium

complexes, the bimetallic complexes out performed their monometallic counterparts for both the ROP of ε-CL, which suggested the presence of beneficial cooperative effects. [7g]

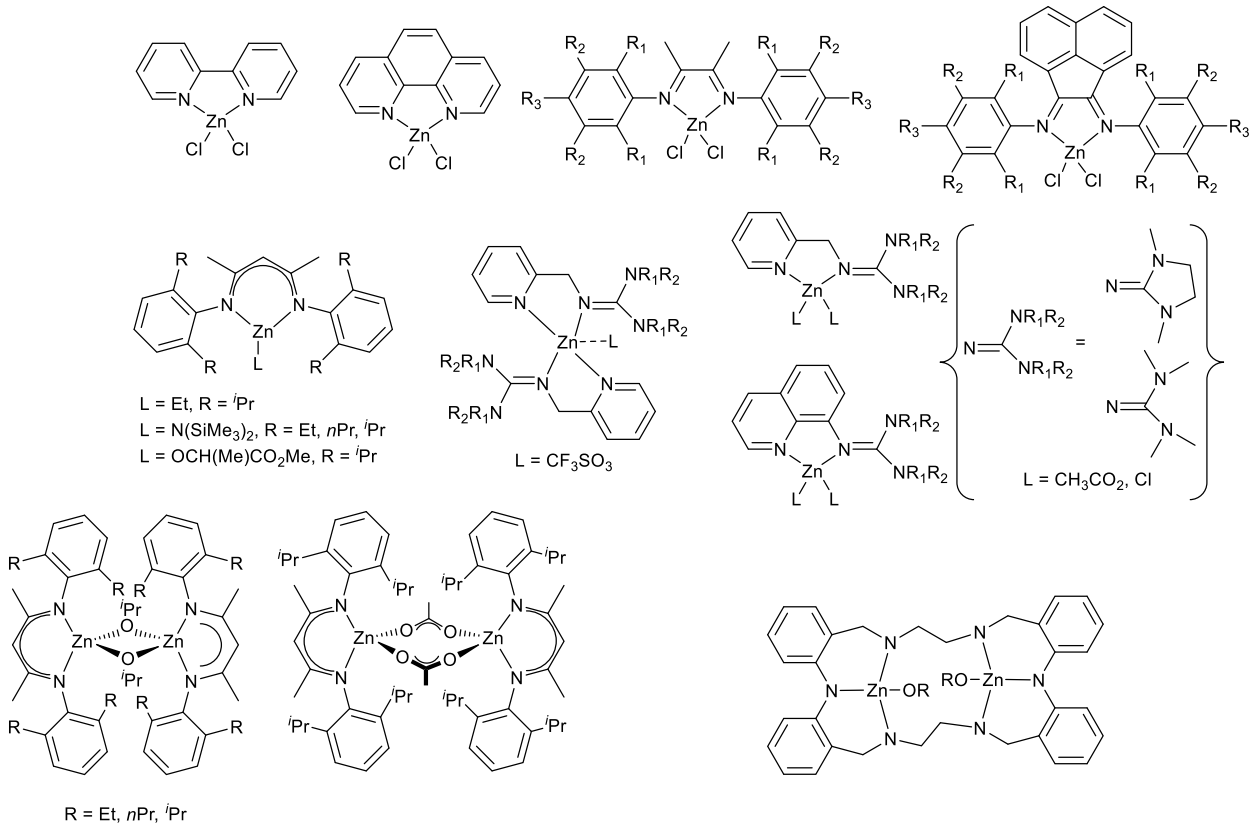

Chart 1. Representative imine-type ligation employed in zinc-based ROP of cyclic esters.

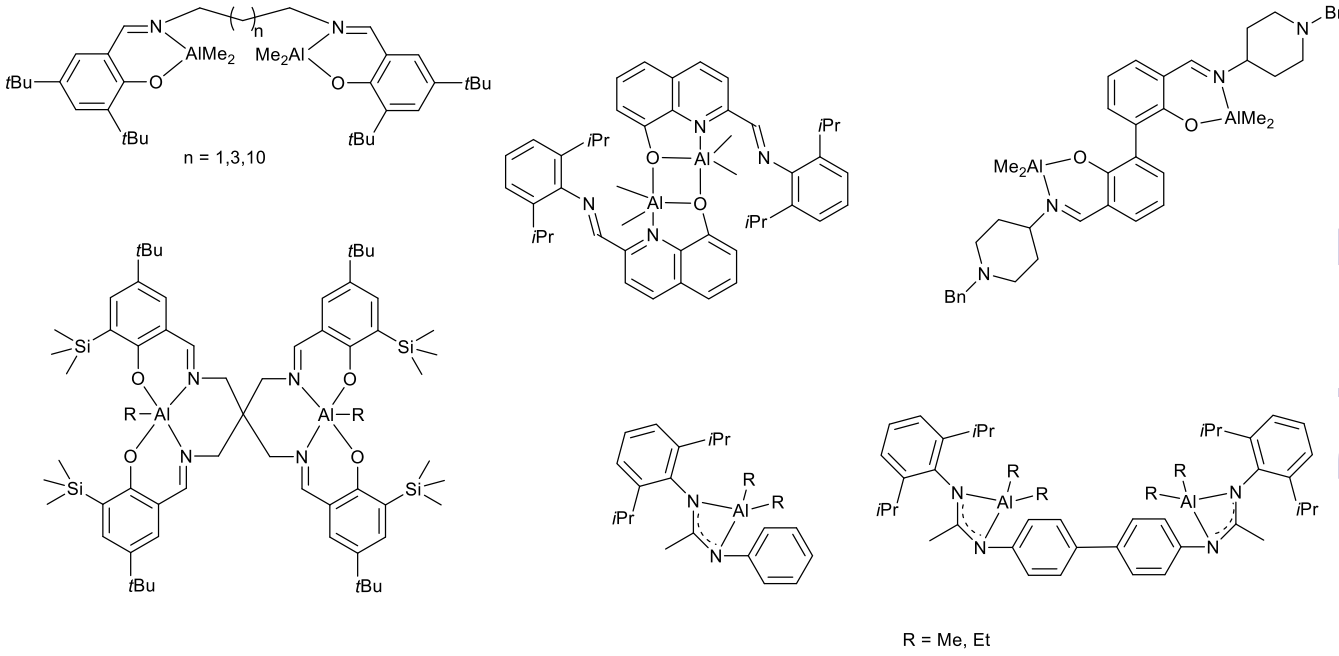

Chart 2. Representative imine-type ligation employed in aluminium-based ROP of cyclic esters.

Also relevant to the work herein is the report by Bochmann *et al*, [7b] who reported that zinc cations bearing the α-diimine (diazadiene) ligand ($MeC{=}NC_6H_3Pr^i_2$-2,6)$_2$, are active for the ROP of ε-caprolactone under mild conditions (60 ^oC, < 1h) but with low conversions (< 13%).

Finally, for this type of α-diimine ligand set, we and others have found that such ligation can, in the presence of alkali metals, aid in the stabilization of metal–metal bonded species. [8] Moreover, low-valent Al^{II}–Al^{II} species bearing α-diimine ligation have been shown to be active catalysts for ε-caprolactone polymerization, and were found to be highly active, which was proposed to be due to the cooperative role between the two Al(II) centers. [8j]

The molecular structures and ROP capability towards the cyclic esters ε-caprolactone (ε-Cl), δ-valerolactone (δ-VL) and *rac*-lactide (*r*-LA) of the complexes **1**–**9** (Chart 3), which are prepared from the pre-ligands $\mathbf{L}^{i\mathbf{Pr}}$, $\mathbf{L}^{\mathbf{Et}}$, $\mathbf{L}^{\mathbf{Me}}$, $\mathbf{L}^{\mathbf{Et\text{-}NO}}$, $\mathbf{L}^{i\mathbf{Pr\text{-}NO}}$, $\mathbf{L}^{i\mathbf{Pr\text{-}N4}}$ and $\mathbf{L}^{i\mathbf{Pr\text{-}N2\text{-}ArCH2Ar\text{-}N2}}$, are reported herein. The effect of the presence of these reduced α-diimines on the ROP process has also been evaluated herein. The interest in the area is stimulated by the application of poly(caprolactone)/poly(lactide) type biodegradable polymers in the packaging and medical arenas. [9]

Results and Discussion

Aluminium complexes

The α-diimines $\mathbf{L}^{i\mathbf{Pr}}$, $\mathbf{L}^{\mathbf{Et}}$ and $\mathbf{L}^{\mathbf{Me}}$ were prepared by standard condensation route as reported in the literature. [10] Subsequent treatment with $AlMe_3$ in refluxing toluene afforded the complexes {$AlMe_2$[$ArNCMe_2C(Me){=}NAr$]} (Ar = 2,6-iPr$_2$C$_6$H$_3$ **1**, 2,6-Et$_2$C$_6$H$_3$ **2**, 2,6-Me$_2$C$_6$H$_3$ **3**, Scheme 1); the structure of {$AlMe_2$[$ArNCH_2C(Me){=}NAr$]} (Ar = 2,6-iPr$_2$C$_6$H$_3$ CCDC number: 709826) has previously been reported, and can be prepared either via direct treatment of the parent diamine with trimethylaluminum (TMA), [4b] or via the reaction of $\mathbf{L}^{i\mathbf{Pr}}CuCl_2$ with $AlMe_3$. [4h]

View Article Online
DOI: 10.1039/C9DT04332B

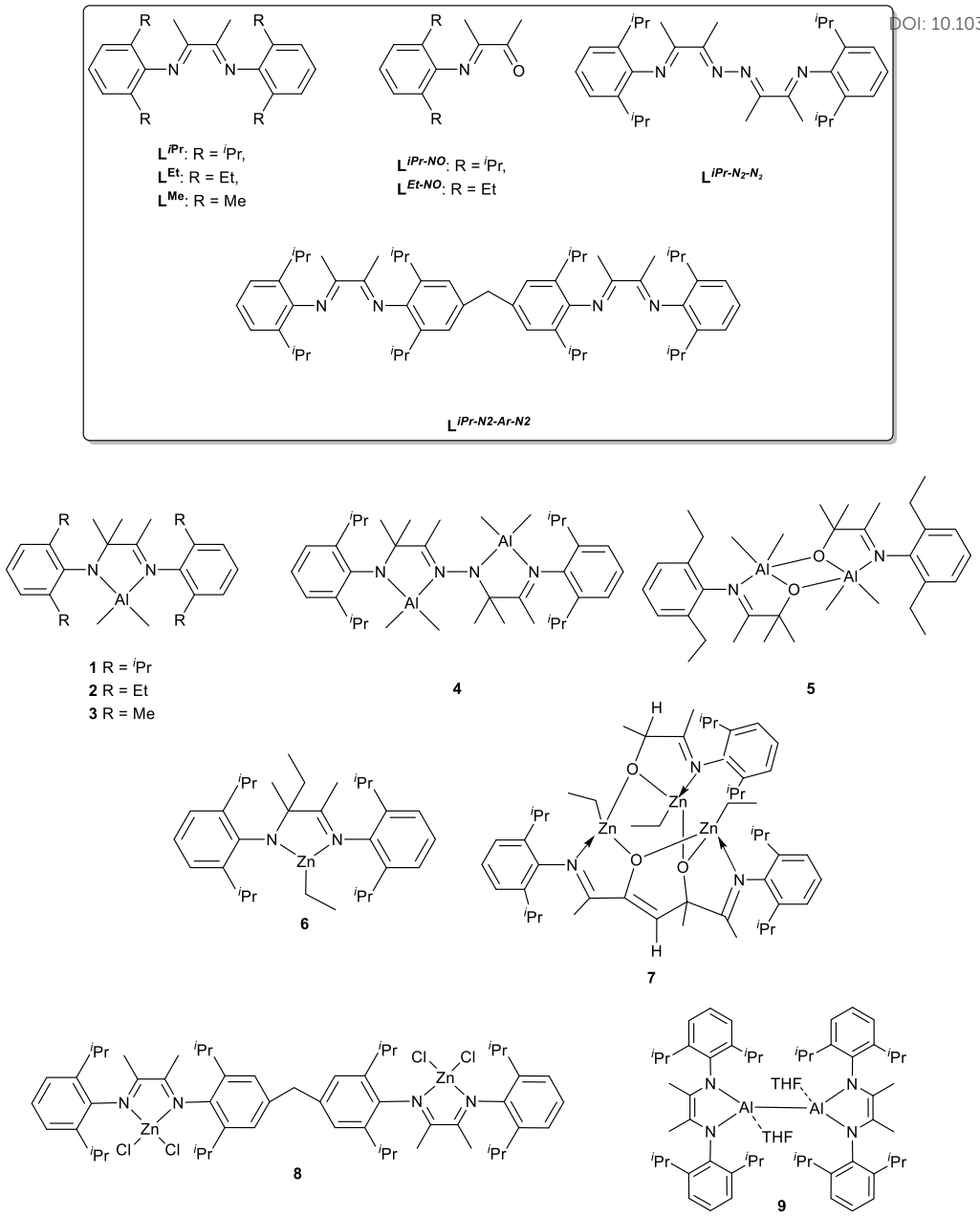

Chart 3. Ligands and complexes investigated herein.

Herein, we have also structurally characterized the related complexes **1**–**3**, which are shown in Figure 1 and Figure S3; selected bond lengths and angles, as well as the values of the four-coordinate geometry index τ_4, [11a] are given in Table 1. In each case, the distorted tetrahedral aluminium centre is bound by a chelating imino-amido ligand. The N1–C1–C2–N2 portion of the imino-amido ligand is almost planar, with an average torsional angle of 3.43º (for **1**), 0.55º (for **2**) and 5.44º (for **3**). The aluminum atom lies within this plane with the greatest deviation observed for **3** (Al atom displaced *ca.* 0.024 Å

(for **1**), 0.033 (for **2**) and 0.16 (for **3**) out of the plane.), with each adopting a distorted tetrahedral geometry (bound by two methyl groups and two nitrogens of the chelating amido–imino ligand). The non-symmetry of structures **1**–**3** is manifested in the different C–N bond distances in the bidentate chelates, whilst the Al–C, Al–N1, Al–N2 and C–N bond lengths found for each of **1**–**3** are similar. As expected, the Al–N bond with the formally negatively charged amido nitrogen N2 is significantly shorter at 1.839(2), 1.845(2) and 1.844(2) Å) Å than the neutral imino nitrogen Al–N1 at 1.986(2), 1.984(3) and 1.988(2) Å for compounds **1**–**3** respectively. The C1–N1 bonds in **1**–**3** (1.286(3), 1.291(4) and 1.295(3) Å are double and are shorter than C2–N2 (1.475(3), 1.467(4) and 1.477(3) Å, respectively). The C1–C2 distances in **1**–**3** (1.508(4), 1.518(4) and 1.502(3) Å are comparable with C–C single bond distances. The sum of the bond angles around the backbone C1 and C2 centers ($\Sigma\angle$C1=360.0º, $\Sigma\angle C_2$ = 435.2º for **1**, $\Sigma\angle$C1=360.0º, $\Sigma\angle C_2$ = 435.7º for **3**, $\Sigma\angle$C1=360.0º, $\Sigma\angle C_2$ = 435.9º for **3**) argue strongly for sp^2 and sp^3 hybridized carbon centers at C1 and C2, respectively.

As noted previously, the ^{1}H NMR spectra for **1**–**3** are consistent with the transfer of one methyl to an imino carbon atom with one singlet for the imino-methyl group at 1.95 (for **1**), 1.93 (for **2**) and 2.03 ppm (for **3**) integrating for three protons and another singlet for the two amino-methyl groups at 1.27 (for **1**), 1.30 (for **2**) and 1.49 ppm (for **3**) integrating for six protons. Characteristic high-field resonances for the aluminum methyl groups are observed at –0.93 (for **1**), –0.95 (for **2**) and –0.78 ppm (for **3**, s, 6H). The presence of the asymmetric amido-imino ligands, causes non-equivalence of the protons of the four isopropyl, ethyl and methyl substituents in each ligand of compounds **1**, **2** and **3** respectively. In complex **1**, the methine protons give rise to two septets (δ = 2.97 and 3.67 ppm) and the methyl groups appear as four doublets (δ = 1.03, 1.07, 1.21 and 1.24 ppm). In complex **2**, the methylene protons give rise to three multiplets (δ = 2.45, 2.65 and 3.08 ppm) and the methyl groups appear as two triplet (δ = 1.18 and 1.24 ppm). In complex **3**, the methyl groups appear as two singlets (δ = 2.31 and 2.50 ppm) (Figures S13–S18). These structures were further investigated by ^{13}C NMR spectroscopy. In particular, the resonances for the aluminum methyl groups (at –7.5, –7.8 and –7.1 ppm for **1**–**3**), amido carbon (67.5, 68.9 and 69.6 ppm for **1**–**3**) and imino carbon (198.6, 197.8

and 197.5 ppm for **1**–**3**) were clearly detected. Furthermore, the presence of the amido-imino chelating fragment in **1**, **2** and **3** is supported by absorptions at 1629, 1659 and 1622 cm^{-1} in their respective IR spectra, which correspond to C=N bonds in their imino-amido skeletons.

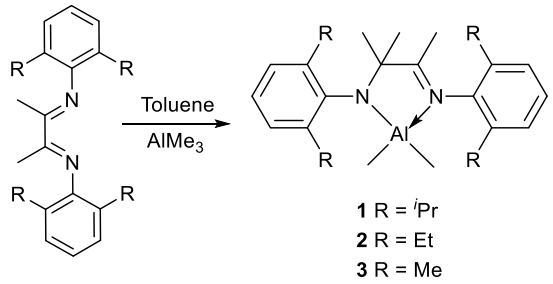

Scheme 1. Synthesis of complexes **1**–**3**.

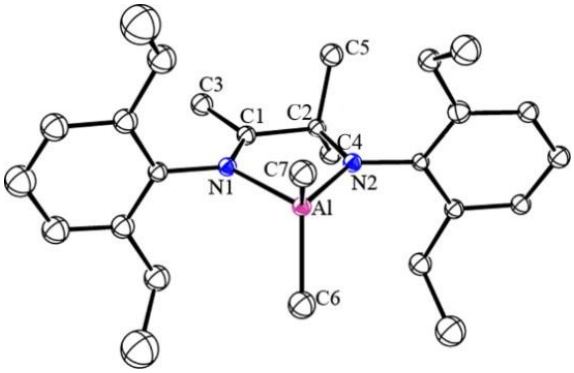

Figure 1. The molecular structure of **1** (top left), **2** (top right) and **3** (bottom) (thermal ellipsoids are set at the 20% probability level; H atoms are omitted for clarity).

Table 1. Selected bond lengths (Å) and angles (°) for compounds **1**–**3**.

	1	**2**	**3**
Al–N1	1.986(2)	1.984(3)	1.988(2)
Al–N2	1.839(2)	1.845(2)	1.844(2)
Al–C6	1.967(3)	1.966(4)	1.967(3)
Al–C7	1.970(3)	1.959(4)	1.965(3)
C1–N1	1.286(3)	1.291(4)	1.295(3)
C1–C2	1.508(4)	1.518(4)	1.502(3)
C1–C3	1.505(4)	1.497(5)	1.506(3)
C2–N2	1.475(3)	1.467(4)	1.477(3)
C2–C4	1.542(4)	1.541(5)	1.554(4)
C2–C5	1.547(4)	1.554(5)	1.543(4)
N1–Al–N2	84.01(1)	84.26(1)	84.68(8)
C6–Al–C7	109.29(2)	109.5(2)	108.23(1)
N1–C1–C2	117.4(2)	117.7(3)	117.53(2)
N2–C2–C1	108.52(2)	107.4(2)	108.52(2)
τ_{4} [10a]	0.94	0.94	0.95

View Article Online
DOI: 10.1039/C9DT04332B

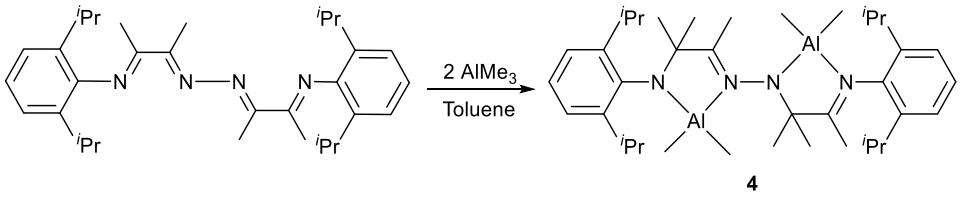

Scheme 2. Synthesis of complex **4**.

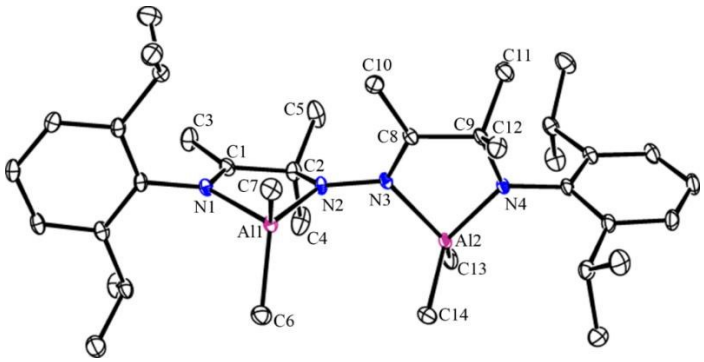

Figure 2. The molecular structure of **4** (thermal ellipsoids are set at the 20% probability level; H atoms are omitted for clarity). Selected bond lengths (Å) and angles (°): Al1–N1 1.971(2), Al1–N2 1.860(2), Al1–C6 1.952(3), Al1–C7 1.956(3), C1–N1 1.306(4), C1–C2 1.516(4), C1–C3 1.493(4), C2–N2 1.454(3), C2–C4 1.549(5), C2–C5 1.515(4), N2–N3 1.430(3), Al2–N3 1.971(2), Al2–N4 1.847(2), Al2–C13 1.966(3), Al2–C14 1.972(3), C8–N3 1.304(3), C8–C9 1.519(4), C8-C10 1.485(4), C9–N4 1.459(4), C9–C11 1.534(4), C9-C12 1.563(4); N2–Al1–N1 82.17(9), C6–Al1–C7 109.47(15), N1–C1–C2 116.9(2), C1–C2–N2 105.3(2), C5–C2–C4 110.1(3), N4–Al2–N3 84.58(9), C13–Al2–C14 120.47(13), N3-C8-C9 116.5(2), C9–C8–C10 119.4(2), C8–C9–N4 108.3(2), C11–C9–C12 107.2(2); Four coordinate geometry index (τ_4) 0.95 (Al1) and 0.85 (Al2). [11a]

The reaction of diacetyl (2,3-butanedione) with 2,6-diisopropylaniline formed 3-(2,6-diisopropylphenylimino)butan-2-one (**L**$^{ipr\text{-}NO}$), which was further reacted with hydrazine to form the bis(α-diimino) ligand (**L**$^{iPr\text{-}N_4}$) bearing two bidentate sites (Scheme 2) and possessing zigzag –N=C–C=N–N=C–C=N-bridging spacers. The molecular structure of ligand **L**$^{iPr\text{-}N_4}$ is shown in Figure S1 of the Supporting Information. The bis(α-diimino) compound (**L**$^{iPr\text{-}N_4}$) was reacted with two equivalents of $AlMe_3$ to form the corresponding asymmetric bi-nuclear aluminium complex $[ArN–C(Me)_2C(Me)=NAlMe_2]_2$ (**4**) as shown in Scheme 2. From the literature, it is known that the reaction of α-diimine compounds with AlR_3 can readily afford imino-amido aluminium compounds or enamine aluminium compounds, resulting from alkyl transfer from aluminium to either the imine carbon atom (C-alkylation) or the imine nitrogen atom (N-alkylation) respectively. [12] Furthermore, the regioselective R-group

transfer step occurring in these reactions is highly dependent on both the metal and the type of R group present in the organometallic reagent. [13] Interestingly, in compound **4**, although both methyl groups attack at the imine carbon, one is found adjacent the Ar group, whilst the other resides on the most distant from Ar. It is thought that the formation of this asymmetric addition product **4** maybe dictated by steric strain imposed by the two amino-methyl groups or isopropyl. Moreover, the compound **4** is *ca*. 18.0 kJ mol^{-1} more stable than the imino-amido isomer derived by the addition of both methyl groups to the imine carbon, that reside on the most distant from Ar, and 30.3 kJ mol^{-1} more stable than the isomer obtained from the addition of both methyls to the imine carbon, that reside adjacent the Ar group (Figure S4, Table S1). The ^{1}H NMR spectrum of **4** is consistent with the molecular structure: the methine protons give rise to two septets (δ = 2.87 and 3.65 ppm) the methyl groups appear as four doublets (δ =1.06, 1.11, 1.21 and 1.27 ppm), and the Al-(CH_3)$_2$ groups are observed as two singlets at –0.81 and –0.75 ppm, respectively (Figures S19 and S20). Noticeably greater bonding asymmetry was also observed, with bond lengths of Al–N(imino) (Al1–N1 1.971(2) and Al2–N3 1.971(2) Å) and Al–N(amido) (Al1–N2 1.860(2) and Al2–N4 1.847(2) Å, Figure 2). The five-membered metallacycle that contains the Al atom adopts a puckered conformation, with the Al atoms residing about 0.406 and 0.323 Å out of the C_2N_2 planes. The angle between the two C_2N_2Al metallacycles is 68.70°. The Al2–C13 (1.966(3) Å) and Al2–C14 (1.972(3) Å) are somewhat longer than those of Al1–C6 (1.952(3) Å) and Al1–C7 (1.956(3) Å). These values are comparable to others reported for Al^{III}–C(sp^3) bond lengths in LAlMe$_2$ type compounds (1.947(4)–2.010(4) Å). [14] In the IR spectra of **4**, there is an intense absorption at 1613 cm^{-1} associated with the C=N stretching mode.

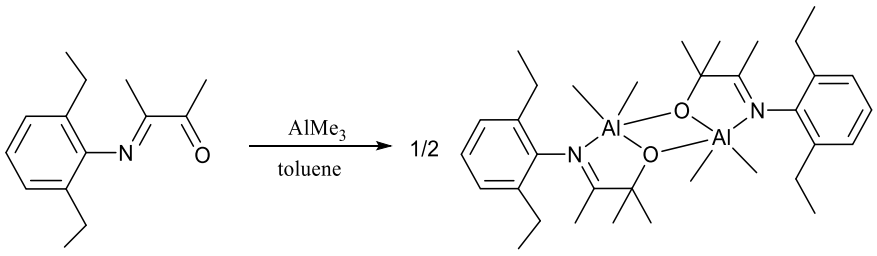

5

Scheme 3. Synthesis of complex **5**.

View Article Online
DOI: 10.1039/C9DT04332B

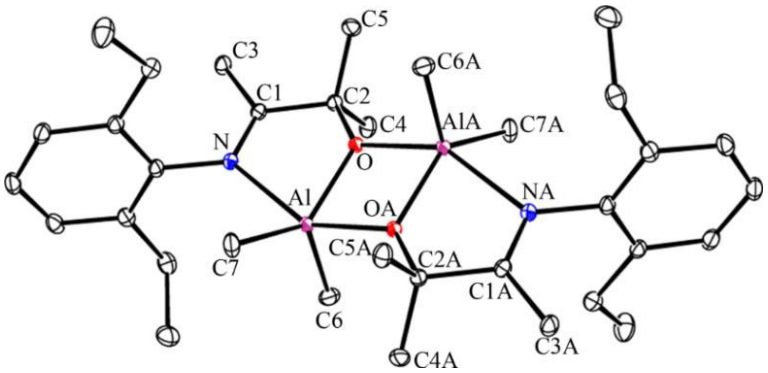

Figure 3. The molecular structure of **5** (thermal ellipsoids are set at the 20% probability level; H atoms are omitted for clarity). Selected bond lengths (Å) and angles (°): Al–N 2.207(1), Al–O 1.849(1), Al–OA 1.962(1), Al–C6 1.984(2), Al–C7 1.987(2), N–C1 1.279(2), C1–C2 1.523(2), C1–C3 1.500(2), C2–O 1.425(2), C2–C4 1.541(2), C2–C5 1.520(2); N–Al–O 76.53(5), C7–Al–C6 119.44(8), O–Al–OA 75.73(5), Al–O–AlA 104.27(5). Five-coordinate geometry index (τ_5) 0.73 (Al). [11b]

Reaction of $\mathbf{L}^{\mathbf{i pr\text{-}NO}}$ with $AlMe_3$ in toluene produces the bimetallic complex $\{[OCMe_2CH(Me)=NAr]AlMe_2\}_2$ (**5**) (Scheme 3). According to the single crystal X-ray diffraction study, complex **5** is a centrosymmetric dimer with a planar Al_2O_2 core (Figure 3), that contains a 5,4,5-fused ring system where Al, N, C1, C2 and O atoms are nearly coplanar with the angle between planes AlNC1C2O and AlOAlAOA being 18.4°. Each aluminium atom is five coordinate and adopts a distorted square-pyramid with a five-coordinate geometry index (τ_5) of 0.73; [11b] the methyl groups C6 are located at the axial positions, whilst C7, N, O and OA are situated in the basal plane. The bond lengths for C(1)–N of 1.279(2) Å and C(1)–O of 1.425(2) Å indicate a localized structure with a C=N double bond and a C–O single bond. The C=N double bond character can be further verified by a very long Al–N distance (2.207(1) Å) indicating a dative bonding from a neutral nitrogen atom to aluminium. The Al−N distance is much larger than in compounds **1–4** having a four-coordinate aluminium (av. 1.982 Å), but comparable with the related compounds with a five-coordinate aluminium (2.136(2)–2.260(3) Å). [15] The shorter Al–O bond (1.849(1) Å) corresponds to a covalent Al–O interaction, whereas the longer one Al–OA (1.962(1) Å) reflects the donor–acceptor bonding, and they are similar to the normal Al–O distance observed for an Al_2O_2 core in the other five coordinate aluminium compounds. [15] The newly formed Al–C6 (1.984(2) Å) and Al–C7 (1.987(2) Å) bonds are almost identical in length. These values are comparable to the Al−C bonds in

compounds **1**–**4** (av. 1.964 Å). Compared to **4**, compound **5** has higher symmetry. The ^{1}H NMR spectra of **5** consists of only one triplet and two multiplets due to the Et groups and only one singlet due to the Al–$(CH_3)_2$ group (Figures S21 and S22). Furthermore, the IR spectrum of compound **5** supports the proposed structure, featuring an intense band due to stretching vibration *ν*C=N bonds (1644 cm^{-1}).

Zinc complexes

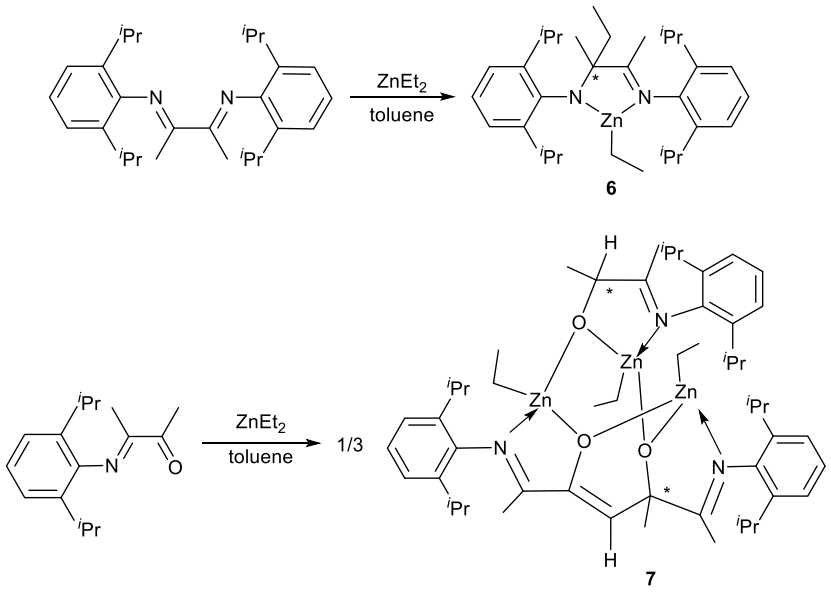

Scheme 4. Synthesis of mono- and tri-nuclear organozinc complexes **6** and **7**.

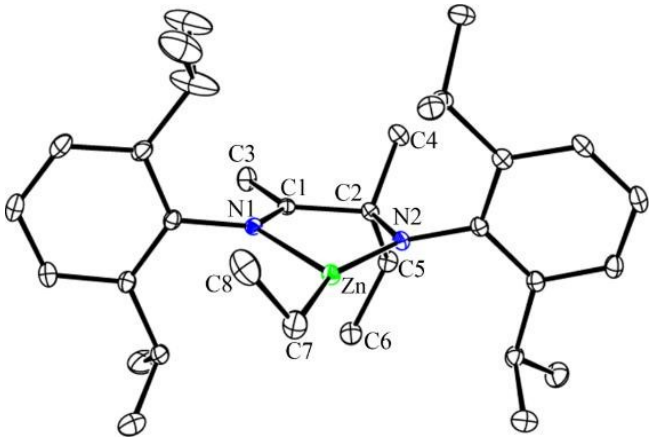

Figure 4. The molecular structure of **6** (thermal ellipsoids are set at the 20% probability level; H atoms are omitted for clarity). Selected bond lengths (Å) and angles (°): Zn–N1 2.106(2), Zn–N2 1.876(2), Zn–C7 1.952(3), N1–C1 1.278(4), C1–C2 1.531(4), C1–C3 1.508(4), C2–N2 1.468(3), C2–C4 1.551(4), C2–C5 1.562(4), C5–C6 1.525(5), C7–C8 1.505(5); N1–Zn–N2 82.11(9), C1–C2–C4 107.3(2), C1–C2–C5 108.2(2), C3–C1–C2 118.6(2).

The reaction of $\mathbf{L}^{i\mathbf{Pr}}$ with $ZnEt_2$ affords **6** via ethyl transfer to an imine carbon of the dpp-dad ligand (Scheme 4). The attachment of an ethyl group to the imine carbon of the chelate ligand generates a chiral center at C2 in molecules of **6** and its symmetry is thus distorted (Figure 4). This situation is reminiscent of chiral amido-imine complexes of zinc and magnesium, with a unit cell containing both isomers (*R* and *S*). [16]

The non-symmetric nature of structure **6** is manifested in the different C−N bond distances for the chelate fragments. The N1–C1 (1.278(4) Å) bond is double and is much shorter than C2–N2 (1.468(3) Å). The Zn–N1 (2.106(2) Å) bond length is remarkably longer than that of Zn–N2 (1.876(2)), reflecting the imino/amido character of the *N*,*N*-chelate and the different bonding situation with donor–acceptor *versus* polar covalent Zn–N interactions. We note that the length of the Zn–C(Et) bond (1.952(3) Å) is somewhat shorter than that observed in LZn-*n*-Bu (where L = [1-*n*-butyl-2-(2,6-diisopropylphenyl)iminoacenaphthen-1-yl]-2,6-diisopropylphenylmide}). [16a] In structure **6**, a five-membered ring ZnN_2C_2 adopts a distorted envelope conformation with the Zn atom displaced *ca*. 0.18 Å out of the ring plane. There is a distorted triangle planar coordination around the Zn center formed by an ethyl group and two nitrogens of the chelating amido-imino.

The reaction of $\mathbf{L}^{i\mathbf{Pr\text{-}NO}}$ with an equimolar amount of the $ZnEt_2$ under similar conditions afforded the trinuclear complex **7** (Scheme 4). A single crystal X-ray structure determination revealed **7** to consist of three different mononuclear units, namely $\mathbf{L}^{i\mathbf{Pr\text{-}NO+H}}$Zn(Et), $\mathbf{L}^{i\mathbf{Pr\text{-}NO\text{-}2H}}$Zn(Et) and $\mathbf{L}^{i\mathbf{Pr\text{-}NO}}$Zn(Et), which result from the abstraction of two hydrogens from one of the methyl groups on the imino unit. Coupling of the imino carbon and the "ex-methyl" carbon of two $\mathbf{L}^{i\mathbf{Pr\text{-}NO}}$ units leads to the formation of the C4–C5 single bond (1.517(7) Å) and generates a chiral center at C5 (Figure 5). The C2–C4 single bond has changed to a C=C double bond (1.351(6) Å), and the mean angle of 120° around the central C4 atom is indicative of a change from sp^3 to sp^2 hybridization due to the elimination of H. The C2–O1 (1.337(5) Å) is between a C=O single bond length (1.43 Å) and a double bond length (1.20 Å), and remarkably shorter than that of C5–O2 (1.427(5) Å), which can be ascribed to an allylic-like delocalization of the negative charge over the C4=C2–O1 fragment. Correspondingly, the C1–C2 bond length

View Article Online
DOI: 10.1039/C9DT04332B

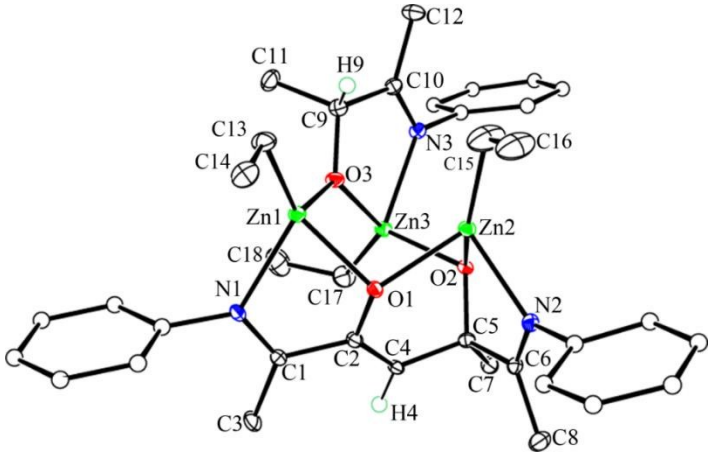

Figure 5. The molecular structure of **7** (thermal ellipsoids are set at the 20% probability level; most of H atoms, *i*Pr groups of L are omitted for clarity; the C atoms in Ph are drawn as smaller spheres). Selected bond lengths (Å) and angles (°): Zn1–N1 2.171(4), Zn1–O1 2.010(3), Zn1–O3 2.035(3), Zn1–C13 1.972(5), N1–C1 1.286(6), C1–C2 1.486(6), C1–C3 1.501(7), C2–C4 1.351(6), C4–H4 0.9500, C2–O1 1.337(5), C4–C5 1.517(7), C13–C14 1.505(8), Zn2–N2 2.131(4), Zn2–O1 2.095(3), Zn2–O2 1.967(3), Zn2–C15 1.965(7), N2–C6 1.282(6), C5–C6 1.528(7), C5–C7 1.533(6), C6–C8 1.507(6), C5–O2 1.427(5), C15–C16 1.437(9), Zn3–N3 2.127(4), Zn3–O2 2.041(3), Zn3–O3 2.028(3), Zn3–C17 1.977(6), N3–C10 1.273(6), C9–C10 1.503(6), C10–C12 1.512(7), C9–C11 1.536(7), C9–H9 1.0000, C9–O3 1.404(5), C17–C18 1.476(8); N1–Zn1–O1 77.09(14), O1–Zn1–O3 86.26(12), N1–Zn1–O3 109.24(14), N2–Zn2–O2 81.21(14), O1–Zn2–O2 88.30(12), N2–Zn2–O2 81.21(14), N3–Zn3–O3 81.21(14), O3–Zn3–O2 99.90(13), N3–Zn3–O2 99.02(13).

(1.486(6) Å) is also somewhat shorter than that of C5–C6 1.528(7) Å). The N1–C1 and N2–C6 bonds are 1.286(6) and 1.282(6) Å and correspond to a C=N double bond. It is also of note that attachment of H to the carbon atom bound to oxygen generates the second chiral center at C9, and the complex molecule adopts a homochiral configuration and the unit cell (Z = 4) consists of two pairs of enantiomers (S_{C5},S_{C9} and R_{C5},R_{C9}).

Complex **7** consists of a six-membered Zn_3O_3 ring with alternating zinc and oxygen atoms, with the Zn atoms each adopting tetrahedral coordination spheres. The conformation of the Zn_3O_3 cycle is a distorted boat, with the Zn2 and O3 atoms at the apices, which is assembled via μ_2-bridging oxygen atoms of the $\mathbf{L}^{\mathbf{iPr\text{-}NO}}$ ligand. The Zn–C bond lengths (mean value 1.972 Å) are comparable and are in the typical range reported for Zn—Me groups. [17] The Zn–O bond lengths vary from 1.967(3) to 2.095(3) Å and compare well with values for Zn–O single bonds found in the other cyclic zinc oxides compounds, such as $[MeZn(bdmap)]_2MeZnOOMe$ and $[MeZn(bdmap)]_2MeZnOH$ (Hbdmap = 1,3-bis(dimethylamino)propan-2-ol). [18] The coordination bond Zn–N1 in

compound **7** (2.171(4) Å) is substantially longer compared to polar covalent Zn–N2 (1.876(2) Å) in compound **6**, but similar with the donor–acceptor Zn–N1 interactions (2.106(2) Å) in **6**. The IR spectrum exhibits an intense absorption band at 1644 cm^{-1}, which corresponds to stretching vibrations of the C=N groups, whilst those associated with C=O double-bond character were lost.

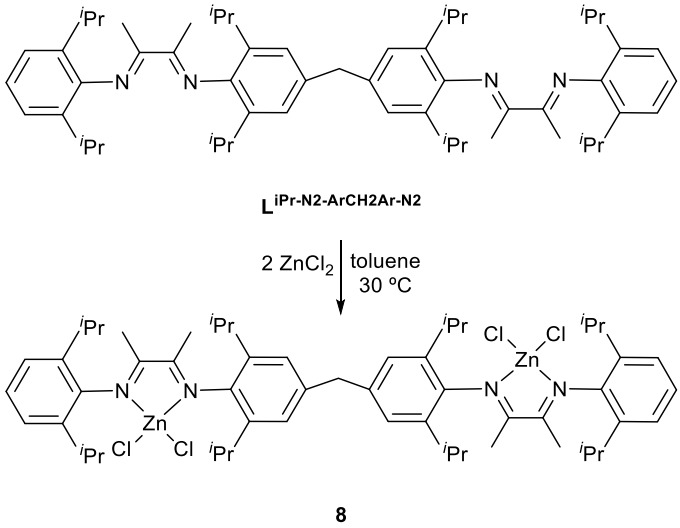

Scheme 5. Synthesis of complexes **8**.

The same method was employed for the synthesis of $\mathbf{L}^{i\mathbf{Pr}\text{-}\mathbf{N_2}\text{-}\mathbf{ArCH_2Ar}\text{-}\mathbf{N_2}}$ as described for the synthesis of $\mathbf{L}^{i\mathbf{Pr}\text{-}\mathbf{N_4}}$, namely 3-(2,6-diisopropylphenylimino)butan-2-one ($L^{i\text{pr-NO}}$) was reacted with 4,4′-methylenebis(2,6-diisopropylaniline) to form the bis(α-diimino) ligand ($\mathbf{L}^{i\mathbf{Pr}\text{-}\mathbf{N_2}\text{-}\mathbf{ArCH_2Ar}\text{-}\mathbf{N_2}}$), which bears two potential bidentate binding sites. [6a] The molecular structure of ligand $\mathbf{L}^{i\mathbf{Pr}\text{-}\mathbf{N_2}\text{-}\mathbf{ArCH_2Ar}\text{-}\mathbf{N_2}}$ is shown in the Supporting Information (Figure S2). The molecule is composed of two equivalent parts connected by atom C3 with the bond angle C7–C3–C7A 121.7(5)º. The C−C 1.505(4) and C=N (1.291(4) Å) distances correspond to single and double bonds, respectively. The two phenyl ring planes, connected through C3, are almost orthorhombic with a dihedral angle between the two rings of 87.8º. This bis(α-diimino) compound $\mathbf{L}^{i\mathbf{Pr}\text{-}\mathbf{N_2}\text{-}\mathbf{ArCH_2Ar}\text{-}\mathbf{N_2}}$ was reacted with two equivalents of $ZnCl_2$ to form the corresponding zinc complex [$\mathbf{L}^{i\mathbf{Pr}\text{-}\mathbf{N_2}\text{-}\mathbf{ArCH_2Ar}\text{-}\mathbf{N_2}}(ZnCl_2)_2$] (**8**) (Scheme 5).

View Article Online
DOI: 10.1039/C9DT04332B

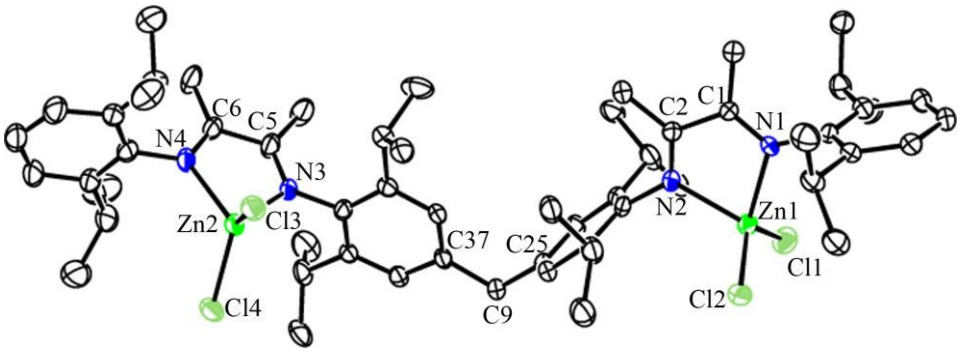

Figure 6. The molecular structure of **8** (thermal ellipsoids are set at the 20% probability level; H atoms are omitted for clarity). Selected bond lengths (Å) and angles (°): Zn1–N1 2.068(4), Zn1–N2 2.081(5), Zn2–N3 2.059(5), Zn2–N4 2.095(6), Zn1–Cl1 2.183(4), Zn1–Cl2 2.194(3), Zn2–Cl2 2.171(5), Zn2-Cl4 2.188(4), C1–C2 1.508(7), C5–C6 1.507(8), C1–N1 1.256(6), C2–N2 1.254(6), C5–N3 1.283(6), C6–N4 1.269(7), N1–Zn1–N2 77.9(2), N3–Zn2–N4 78.93(18), Cl1–Zn1–Cl2 120.30(14), Cl3-Zn2–Cl4 117.04(8), C25–C9–C37 113.6(4). Four-coordinate geometry index τ_4 0.87 (Zn1). [11a]

The molecular structure of complex **8** is shown in Figure 6, with selected bond lengths and angles listed in the caption. Here, one ligand coordinates to two zinc(II) centers, and the molecule is composed of two similar parts connected by C9. Both zinc centers point in the same direction with respect to the ligand framework, and the latter adopts a more pinched structure (C25–C9–C37 at 113.6(4)º), which is somewhat smaller than observed in $\mathbf{L}^{i\mathbf{Pr\text{-}N_2\text{-}ArCH_2Ar\text{-}N_2}}$ (121.7(5)º). Moreover, the dihedral angle between the two aromatic rings connected by C9 in $\mathbf{L}^{i\mathbf{Pr\text{-}N_2\text{-}ArCH_2Ar\text{-}N_2}}$ (87.8º) is much larger than that observed in **8** (78.6º). The metal centers all possess distorted-tetrahedral geometries (τ_4 = 0.87) and deviate slightly (by 0.093 and 0.297Å) from the C_2N_2 planes. The angle between the two C_2N_2Zn planes is 69.0º and the bond distances associated with the $\mathbf{L}^{i\mathbf{Pr\text{-}N_2\text{-}ArCH_2Ar\text{-}N_2}}$ backbone in **8** are virtually identical to those found in the free ligand. The C–N distances, which average 1.265 Å, correspond to C=N bonds, while the C–C separation of 1.508 Å falls in the C–C single bond range. The Zn–N bond lengths (av. 2.076 Å) reflects the donor–acceptor bonding, and is very similar with that in (*t*-Butyl-BIAN)$ZnCl_2$ (2.081 Å) which bears a neutral ligand. [19] The ^{1}H NMR spectrum of **8** is consistent with the molecular structure, *viz* the methine protons give rise to one septet (δ = 2.93 ppm), the methyl groups appear as two doublets (δ =1.13 and 1.35 ppm),

View Article Online
DOI: 10.1039/C9DT04332B

and the methylene is observed as a singlet at 3.98 ppm (Figures S27 and S28).

We have previously reported an Al–Al-bonded compound (dialumane) with an α-diimine ligand, namely [L(THF)Al−Al(THF)L] (**9**), which contains sub-valent Al^{II} centers and dianionic α-diimine ligands (L^{2-}, $(2,6\text{-}i\text{Pr}_2C_6H_3)NC(CH_3)]_2^{2-}$). [8a] Complex **9** can act as a multi-electron donor in the reaction with small molecules, [8a, 20] for example, reaction of **9** with azobenzene derivatives proceeded through a four-electron reduction pathway that involved both the Al^{II} centers and the L^{2-} ligands. [8a]

Reactions involving multielectron transfers between metal centers and substrates are at the core of many important transformations in biology and chemistry. [21] In addition, multimetallic catalysis is based on the combined action of metals in a chemical transformation. It has witnessed rapidly increasing developments during the past decades in numerous areas of chemistry. Close proximity between the metal centers thus appears to provide favourable conditions for the occurrence of enhanced catalytic properties, and this proximity can result from the existence of direct metal−metal interactions. [22] These species have attracted great interest not only because of the novel bonding nature of the low-valent, low-coordinate metal centers, but also because they display fascinating reactivity toward a variety of small molecules as well as potential applications in catalysis. [23, 8j] Encouraged by this multi-electron-reduction property of dialumane **9**, and the recent results reported by Fedushkin, Dagorne *et al* on related Al–Al bonded complexes bearing acenaphthenequinonediamido ligation, [8j] we also included **9** as a potential catalyst in our studies on the ring opening polymerization (ROP) of the cyclic esters ε-caprolactone (ε-Cl), δ-valerolactone (δ-VL) and *rac*-lactide (*r*-LA), see next section.

Ring Opening Polymerization (ROP) of Cyclic Esters

ε-Caprolactone (ε-CL)

The Al- and Zn-based complexes prepared herein were tested as catalysts for the ROP of ε-CL (Table 2). At 30 °C, good conversions were achieved in the presence of complexes **1**–**3** over 60 min (runs 1–4), with the R = *i*-Pr (**1**) and Me (**3**) systems outperforming the

R= Et (**2**) system in terms of both conversion and control. The bimetallic system **4** (which is an *i*-Pr derivative) afforded only slightly higher conversion than **1** (91 *vs* 89%, *cf*. runs 1 and 4), but with far less control (2.10 *vs* 1.20). On the other hand, longer reaction times were required by the bimetallic species **5** (an ethyl derivative) in order to obtain complete conversion (480 min *versus* 60 min, runs 5 and 6). In the case of the Zn-based catalysts **6** and **7** (runs 7 and 8), mono-metallic **6** (an *i*-Pr derivative) afforded 84% conversion (run 7) with good control (1.20), whilst tri-metallic **7** (also an *i*-Pr derivative) afforded near quantitative conversion (99%) but with slightly less control (1.70). Interestingly, almost no activity was observed in the presence of the Zn species **8** (run 9). We ascribe this inactivity to the inefficient formation of the required catalytically active alkoxide species from this chloride pre-catalyst. Indeed, we note that in reports by other groups, the formation of M-OR species from parent a chloride complex required salt metathesis via the use of Na (or K) alkoxides, rather than by direct reaction with alcohols. [24] Concerning the effect of the metal center (zinc *versus* aluminium), slightly lower conversions and polymer M_n were observed in the presence of the Zn-species **6** at 30 ºC, compared to the values obtained when using the Al-derivative **1** (*cf*. runs 7 and 1). Notably, the Al-Al bonded complex **9** outperformed all the other systems tested herein, allowing for complete monomer conversion within 5 minutes (run 10). No drop in activity was observed on progressively increasing the monomer/catalyst ratio from 100 to 2000 in the presence of different amounts of co-catalysts (runs 11-14). Whilst the *modus operandi* of this catalysts is not clear, work by Fedushkin, Dagorne *et al*, supported by DFT studies, suggests the Al(II)–Al(II) bond is not cleaved during the catalytic process and the alcohol coordinates one of the metal centres leading, *via* proton transfer to a nitrogen atom of the ligand, to an Al(II)-alkoxide species. [8j] Preliminary ROP studies conducted in the absence of BnOH reveal a clear reduction in activity (conversion 44% over 15 min.), suggesting the alcohol is indeed playing a role here. [25] In the case of catalysts **1**–**3** and **6**, the M_n of the isolated polymers was lower than the calculated values albeit with narrow polydispersities. Broader M_w/M_n (spanning from 1.7 to 2.6) were obtained in the case of the multimetallic species **4**, **5** and **7**, suggesting the occurrence of transesterification reactions between the two (or three, in the case of **7**) metal centers. In spite of the broader

polydispersities, conversions and M_n values achieved by using **9** were found to be higher than those obtained in the presence of the dialumane complex reported by Fedushkin, Dagorne *et al* under the same reaction conditions. [8j]

By increasing the temperature to 80 °C, all complexes exhibited increased activity with high conversions achieved in most cases within minutes. In particular, only 1 minute was required in the presence of complex **9** (run 27) to achieve quantitative conversion. In all cases, M_n values lower than the expected were obtained. Compared to the experiments carried out at 30 °C, a broadening of molecular weight distribution, thought to be due to increased transesterification, was observed. These results highlighted several differences in the catalytic behavior of the complexes, for example, the bimetallic complex **4** allowed for significantly higher molecular weight albeit with less control (*cf.* runs 15 and 18) *versus* **1**. However, in terms of catalytic conversion, the appeared to be little benefit from the presence of the second metal. Noteworthy, comparable results for zinc *versus* aluminium were observed at higher temperature (*cf.* runs 15 and 25). Regardless of the reaction temperature, narrower polydispersities were achieved in the presence of the Zn catalyst.

Table 2. ROP of ε-CL promoted by complexes **1**–**9**.

Run	Cat.	ε-CL:M:BnOH	T °C	t min	Conv. (%)[a]	M_n[b,c] (kDa)	M_{nCalcd}[d] (kDa)	PDI[b]
1	**1**	250:1:1	30	60	89	13.0	25.6	1.20
2	**2**	250:1:1	30	60	78	19.2	22.2	1.30
3	**3**	250:1:1	30	60	89	19.1	25.4	1.20
4	**4**	250:1:1	30	60	91	12.8	26.0	2.10
5	**5**	250:1:1	30	60	29	0.4	8.40	2.10
6	**5**	250:1:1	30	480	>99	17.3	28.6	2.70
7	**6**	250:1:1	30	60	84	11.2	24.1	1.20
8	**7**	250:1:1	30	60	99	15.1	28.5	1.70
9	**8**	250:1:2	30	60	2	nd	nd	nd
10	**9**	250:1:1	30	5	>99	28.1	29.6	1.30
11	**9**	100:1:1	30	15	96	22.5	11.1	1.10
12	**9**	1000:1:10	30	10	92	16.9	10.6	1.20
13	**9**	1000:1:3	30	10	93	55.5	35.3	1.80
14	**9**	2000:1:3	30	10	87	56.0	66.2	1.60

View Article Online
DOI: 10.1039/C9DT04332B

15	**1**	250:1:1	80	5	94	11.7	27.0	1.70
16	**2**	250:1:1	80	5	94	23.4	27.0	1.30
17	**3**	250:1:1	80	5	98	20.4	28.1	1.50
18	**4**	250:1:1	80	5	94	21.0	27.0	2.70
19	**4**	125:1:1	80	30	>99	8.10	14.4	1.90
20	**4**	250:1:1	80	30	>99	16.3	28.6	2.20
21	**4**	500:1:1	80	30	88	20.3	50.2	2.20
22	**4**	1000:1:1	80	30	21	16.4	23.7	2.10
23	**5**	250:1:1	50	80	99	20.4	28.5	1.20
24	**5**	250:1:1	80	5	30	23.7	8.80	2.70
25	**6**	250:1:1	80	5	94	11.4	27.0	1.10
26	**7**	250:1:1	80	5	>99	9.40	28.5	2.00
27	**9**	250:1:1	80	1	>99	10.6	28.5	1.20

[a] Determined by ^{1}H NMR spectroscopy on crude reaction mixture. [b] From GPC. [c] Values corrected considering Mark–Houwink factor (0.56) from polystyrene standards in THF. [d] Calculated from ($[Monomer]_0/[OH]_0$) × conv. (%) × Monomer molecular weight + Molecular weight of BnOH.

δ-valerolactone (δ-VL)

The ROP of δ-VL was next investigated (Table 3). In the presence of the Al-based complexes **1**–**4** and **9**, high conversions spanning from 88 to > 99% were achieved in 4 h at 30 °C (runs 1–4 and 8). As for ε-CL, the R = Et derivative (**2**) was less active here than the *i*-Pr (**1**) and Me (**3**) derivatives. The mono-Al species **1**–**3** and the bimetallic compound **4** were found to be equally performing in terms of monomer conversion. Nevertheless, the polymer molecular weight obtained in the presence of **4** (*i*Pr) was found to be *ca*. 2-fold higher than that of the material isolated with the monometallic complex **1** (*i*Pr) at 30 ºC (23 kDa *vs* 11kDa, runs 4 and 1, respectively). Low monomer conversion (35%) was observed when compound *N*,*O*-chelate bimetallic complex **5** was employed (run 5). Both Zn-based species **6** and **7** exhibited good activity, allowing for 80 and 99% conversion, respectively (runs 6 and 7), suggesting that, unlike for Al (**5**), the presence of the *N*,*O*-chelate is not detrimental. However, direct comparisons are difficult given **7** is trimetallic and an *i*-Pr derivative *versus* bimetallic **5** (an Et derivative). Similarly to the case of ε-CL, shortened reaction times were required when performing the reaction at 80 °C instead of 30 °C (runs 9–14 and 17–22). Indeed, almost complete conversion was achieved with complexes **1**–**4** and **9** and **6**–**7** within 15 minutes. Compared to the other catalysts, complex **5** proved to be less active, requiring longer reaction time for complete

monomer conversion even at higher temperature (runs 15–17). In all cases, M_n values lower than the expected were observed, and polydispersities spanned the range 1.1 to *ca*. 2. Notably, complex **5** afforded oligomeric species (M_n = 500) both at 30 and 80 °C (runs 5 and 17, respectively), which suggested inefficient catalyst activation in the former case and early deactivation in the latter. The reactivity trend of the catalysts was found to be similar to that observed in the case of the ROP of ε-CL.

On increasing the temperature to 80 ºC, monometallic **1** – **3** exhibited similar catalytic performances to the bimetallic system **4** and afforded polymers with comparable M_n values. In general, slightly better control was exhibited by the monometallic compounds (M_w/M_n 1.40 *vs* 1.70, runs 9 and 14, respectively). The *N*,*O*-chelate bimetallic complex **5** required longer reaction times to achieve high conversion, with slightly better results achieved in the presence of BnOH. The mono-Zn species **6** performed better in the presence of excess BnOH (two equivalents), albeit with slightly worse control. In the presence of one equivalent of BnOH, the tri-metallic compound **7** afforded a higher conversion *versus* **6**, but with slightly poorer control. In turn, complex **6** was found to be slightly less active than the Al-derivative **1** at 80 ºC. When the reaction was performed at room temperature, the system **1** allowed for better conversions and higher polymer M_n, as well as for narrower polydispersity (*cf*. runs 1 and 6).

Table 3. ROP of δ-VL promoted by compounds **1–9** (not **8**).

Run	Cat.	δ-VL:M:BnOH	T/ °C	t min	Conv. (%)[a]	M_n[b] (kDa)	M_{nCalcd}[c] (kDa)	PDI[b]
1	**1**	250:1:1	30	240	98	11.0	24.6	1.10
2	**2**	250:1:1	30	240	83	14.9	20.8	1.40
3	**3**	250:1:1	30	240	97	16.2	24.4	1.60
4	**4**	250:1:1	30	240	99	22.8	24.9	1.70
5	**5**	250:1:1	30	240	35	0.50	8.70	1.60
6	**6**	250:1:1	30	240	81	6.50	22.1	1.20
7	**7**	250:1:1	30	240	99	14.8	24.9	1.70
8	**9**	250:1:1	30	240	>99	23.2	25.1	1.60
9	**1**	250:1:1	80	15	93	15.6	23.5	1.40
10	**1**	250:1:1	80	20	98	12.8	24.6	1.70
11	**1**	250:1:2	80	20	98	13.4	24.6	2.00
12	**2**	250:1:1	80	15	94	11.8	23.7	1.50

13	**3**	250:1:1	80	15	95	16.1	23.1	1.50
14	**4**	250:1:1	80	15	94	16.9	23.7	1.70
15	**5**	250:1:0	50	240	93	22.2	23.5	1.80
16	**5**	250:1:1	50	240	>99	19.6	25.0	1.50
17	**5**	250:1:1	80	15	61	0.50	15.1	1.70
18	**6**	250:1:1	80	15	83	16.8	20.1	1.50
19	**6**	250:1:2	80	15	97	10.9	24.4	1.70
20	**7**	250:1:1	80	15	98	12.2	24.6	1.70
21	**9**	250:1:1	80	15	98	10.1	24.7	1.60
22	**9**	250:1:2	80	15	99	16.8	12.5	1.70

[a] Determined by ^{1}H NMR spectroscopy on crude reaction mixture. [b] From GPC. [c] Calculated from ([Monomer]$_0$/[OH]$_0$) × conv. (%) × Monomer molecular weight + Molecular weight of BnOH.

By increasing the temperature, comparable molecular weights were obtained, although higher conversion was achieved in the presence of the Al-based complex. Interestingly, the polydispersity was shown to be dependent on the amount of co-catalyst employed. Also for ε-CL, the M–M bonded complex **9** outperformed the other catalysts, particularly at 30 ºC.

rac-Lactide (r-LA)

The ROP of *rac*-lactide (*r*-LA) promoted by the Al-based catalysts was then undertaken (Table 4). Moderate conversions were obtained in the presence of all complexes (runs 1–10) at both 30 and 80 ºC. However, liquid oligomers whose M_n could not be detected by GPC were obtained in all cases, regardless of the reaction conditions employed. There was little variation in activity for **1** – **3**, and the bimetallic system **4** performed no better. A slightly enhanced conversion was achieved using the *N*,*O*-chelate bimetallic complex **5**, whilst activity similar to that of **1** – **4** was displayed by the Al-Al bonded complex **9**. Use of the Zn-based complexes (Table 5) led in general to better performances. In the presence of monometallic **6**, 50% monomer conversion was achieved at 30 ºC, affording low molecular weight oligomers (run 1). An improvement was observed by increasing the temperature to 80 ºC (run 2). Indeed, 66% conversion was obtained in 10 min., affording PLA with M_n of *ca*. 10 kDa; trimetallic complex **7** displayed similar activity at 30ºC over

Table 4. ROP of *r-LA* promoted by Al compounds **1–5** and **9**.

Run	Cat.	*r*-LA:M:BnOH	T□	t min	Conv. %[a]	M_{nCalcd}[b] (KDa)	Products

1	**1**	250:1:1	30	240	44	15.8	oligomers
2	**1**	250:1:1	80	10	52	18.8	oligomers
3	**2**	250:1:1	30	240	48	17.4	oligomers
4	**2**	250:1:1	80	10	45	16.3	oligomers
5	**3**	250:1:1	30	240	51	18.5	oligomers
6	**3**	250:1:1	80	10	49	17.7	oligomers
7	**4**	250:1:1	30	240	50	18.1	oligomers
8	**4**	250:1:1	80	10	47	17.0	oligomers
9	**5**	250:1:1	80	50	64	23.0	oligomers
10	**9**	250:1:1	80	10	52	18.8	oligomers

[a] Determined by ^{1}H NMR spectroscopy on crude reaction mixture. [b] Calculated from ([Monomer]$_0$/[OH]$_0$) × conv. (%) × Monomer molecular weight + Molecular weight of BnOH.

over 4 h, affording a polymer with molecular mass significantly lower than the calculated value (see Table 5, Run 3). Nevertheless, by increasing the temperature to 80 ºC, higher conversion (69%) and M_n were obtained (run 4). The syndiotactic bias (P_r) of the PLA was determined by homonuclear 2D-J resolved ^{1}H NMR spectroscopy. [26] Isotactic polymers were obtained in all cases (P_r values spanning from 0.20 to 0.30).

Table 5. ROP of *r-LA* promoted by Zn compounds **6** and **7**.

Run	Cat.	*r*-LA:M:BnOH	T □	t min	Conv. %[a]	M_n[b] (kDa)	M_{nCalcd}[c] (kDa)	PDI[b]	P_r
1	**6**	250:1:1	30	240	50	nd	18.2	nd	nd
2	**6**	250:1:1	80	10	66	9.80	23.1	2.00	0.22
3	**7**	250:1:1	30	240	65	3.70	23.6	2.30	0.34
4	**7**	250:1:1	80	10	69	5.80	24.8	1.70	0.19

[a] Determined by ^{1}H NMR spectroscopy on crude reaction mixture. [b] Calculated from ([Monomer]$_0$/[OH]$_0$) × conv. (%) × Monomer molecular weight + Molecular weight of BnOH.

Co-polymerization of ε-CL and δ-VL

Finally, the co-polymerization of ε-CL with δ-VL was examined (Table 6). In the presence of complex **1**, moderate conversion was observed by conducting the reaction at 30 ºC, while an enhancement was obtained on increasing the temperature to 50 ºC (54 to 85 %, runs 1 and 2, respectively). The formation of low molecular weight oligomers was achieved by using **2** at 30 ºC (run 3), while a co-polymer with M_n >7,800 was isolated in the reaction performed at higher temperature (run 4). Similar behaviour was exhibited also by complex **3** (runs 5 and 6). Notably, these three catalysts revealed a slight preference for the incorporation of ε-CL over the other co-monomer. Complete

conversion of both monomers was observed by using the bimetallic compound **4** (run 7), while liquid oligomers were isolated using complex **5** (run 8). Similarly to **1** – **3**, complex **5** displayed a higher propensity towards the incorporation of ε-CL over δ-VL, while a co-polymer with a 1:1 CL/VL ratio was isolated in the presence of **4**, as observed by ^{1}H NMR spectroscopy (70:30 *versus* 50:50, runs 8 *versus* 7). The bimetallic species **4** (*i*Pr) was shown to be better performing than its mono-Al congener **1** (*i*Pr), allowing for better conversion and higher polymer M_n (cf. runs 1 and 7). Moreover, the amount of δ-VL incorporated in the co-polymer was found to be higher than that of the product isolated in the presence of **1** (50% and 40%, respectively). In the case of the Zn-based catalysts, low molecular weight products were isolated in the presence of monometallic **6** at 30 ºC (run 9). Nevertheless, by increasing the temperature, improvements of monomer conversion and polymer molecular weight were achieved (run 10). In the case of trimetallic **7**, high conversions were obtained both at 30 and 50 ºC (runs 11 and 12, respectively). Monometallic complex **6** proved to preferentially incorporate ε-CL, regardless of the reaction temperature. Notably, in the presence of trimetallic catalyst **7**, the tendency to incorporate δ-VL improved on increasing the temperature. Concerning to the effect of the metal center, the ε-CL incorporation was found to be higher in the co-polymers synthesized with the Zn-based complex **6** than in those obtained in the presence of the Al system **1** (50 *vs* 40%, respectively). Finally, full consumption of both monomers was achieved in the presence of the dialumane system **9**, regardless of the reaction conditions (runs 13 and 14).

Table 6. Co-ROP of ε-CL and δ-VL using compounds **1** - **9** (not **8**).

Run	Cat.	ε-CL:δ-VL:M:BnOH	T ºC	t min	ε-CL:δ-VL[a]	Conv. %[a]	M_n[b,c] (kDa)	PDI[b]
1	**1**	250:250:1:1	30	180	60:40	54	9.40	1.70
2	**1**	250:250:1:1	50	60	62:38	85	11.2	1.70
3	**2**	250:250:1:1	30	180	65:35	41	oligomers	
4	**2**	250:250:1:1	50	60	58:42	69	7.80	1.50
5	**3**	250:250:1:1	30	180	73:27	39	oligomers	
6	**3**	250:250:1:1	50	60	47:53	84	22.4	1.70
7	**4**	250:250:1:1	50	60	50:50	98	18.6	1.80

8	**5**	250:250:1:1	50	60	72:28	52	oligomers	
9	**6**	250:250:1:1	30	180	78:22	34	oligomers	
10	**6**	250:250:1:1	50	60	75:25	62	12.3	1.80
11	**7**	250:250:1:1	30	180	65:35	85	9.40	2.00
12	**7**	250:250:1:1	50	60	50:50	>99	22.5	1.90
13	**9**	250:250:1:1	30	120	50:50	99	8.30	1.90
14	**9**	250:250:1:1	50	10	50:50	>99	18.4	1.80

[a] Determined by ^{1}H NMR spectroscopy. [b] From GPC. [c] Values corrected considering the Mark-Houwink factor (M_n × 0.56 x %$_{CL}$+ M_n x %$_{VL}$) from polystyrene standards in THF.

Kinetic studies

A kinetic study of the ROP of δ-VL using **1**, **4** and **6** highlighted that the polymerization rate exhibited a first order dependence on the monomer concentration (Figure 7, left), and the conversion of monomer achieved over 60 min was > 75% (90% for **4**). The activity trend was found to be **4** ≈ **1** > **6**.

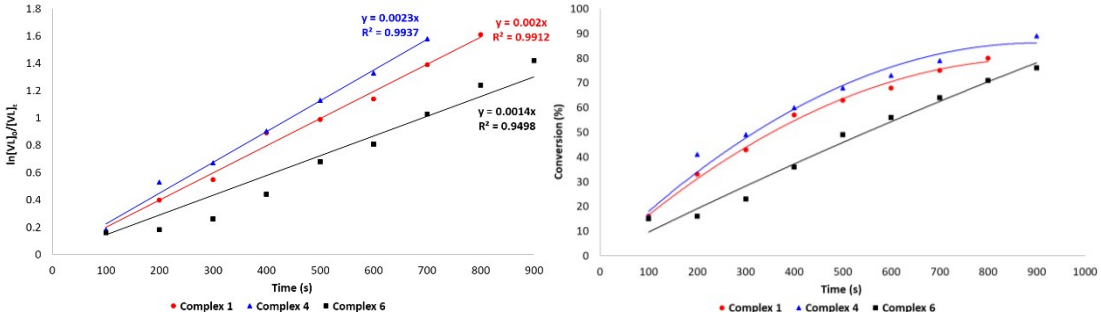

Figure 7. Left: Plot of ln[VL]$_0$/[VL]$_t$ *vs.* time using complex **1**, **4** and **6**; right: relationship between conversion and time for the polymerization of VL.

In conclusion, we have isolated and structurally characterized a number of aluminum, zinc and gallium species bearing α-diimine and related ligand sets. The known alkyl transfer chemistry of organoaluminium and zinc towards α-diimines was exploited in related aluminium bis(α-diimine) chemistry, and then extended to related acetylimino zinc and aluminium systems. In the case of zinc, an unusual trinuclear complex {[ArN=C(Me)COCHCO(Me)C(Me)=NAr][OCH(Me)C(Me)=NAr](ZnEt)$_3$} (Ar = 2,6-*i*Pr$_2$C$_6$H$_3$, **7**) was identified. All complexes, together with a previously reported Al-Al bonded dialumane complex, were tested as catalysts in the ROP of cyclic esters. Concerning the hompolymerization of ε-CL and δ-VL, complexes **1** (*i*Pr) and **3** (Me) proved to be better performing than **2** (Et), while the bimetallic compound **4** slightly

outperformed its analog **1**. The bimetallic Al species **5** was shown to be far less active. In fact, only low molecular weight oligomers were obtained under the optimized reaction conditions. Compared to the monometallic Zn species **6**, the trimetallic complex **7** allowed for higher monomer conversions albeit with less control. The Cl-bearing complex **8** was found to be almost inactive in the ROP of ε–caprolactone, which was thought to be due to activation problems. By contrast, the low-valent Al(II)–Al(II) system **9** proved to be the best catalyst amongst those tested herein, and allowed for the complete conversion of the monomer at lower temperatures and/or shorter reaction times than required by the other systems herein. Notably, the activity of this complex in the ROP of ε-CL was found to be comparable to that of a recently disclosed species having the same type of M–M bond. [8j] This work and that of Fedushkin, Dagorne *et al* [8j] suggests that for this type of ligation, the presence of the M-M bond is highly beneficial in terms of activity and cooperation between the metal centres. A similar activity trend was observed in the CL/VL co-polymerization and all catalysts proved to preferentially incorporate CL over the other co-monomer. Concerning the polymerization of *r*-LA, oligomers were isolated when using the aluminum-based complexes, while isotactic PLAs were obtained in the presence of the zinc catalysts **6** and **7**.

Experimental

General: All manipulations were carried out under an atmosphere of dry nitrogen using conventional Schlenk and cannula techniques or in a conventional nitrogen-filled glove box. Hexane and toluene were refluxed over sodium. All solvents were distilled and degassed prior to use. The α-diimine ligand $\mathbf{L}^{\mathbf{i pr}}$, $\mathbf{L}^{\mathbf{Et}}$, $\mathbf{L}^{\mathbf{Me}}$ and $\mathbf{L}^{\mathbf{i pr\text{-}NO}}$, $\mathbf{L}^{\mathbf{Et\text{-}NO}}$, $\mathbf{L}^{\mathbf{i Pr\text{-}N_4}}$ and $\mathbf{L}^{\mathbf{i Pr\text{-}N_2\text{-}ArCH_2Ar\text{-}N_2}}$ were prepared according to literature procedures. [6a, 10, 27] Trimethylaluminium ($AlMe_3$) and diethyl zinc ($ZnEt_2$) and hydrazine (H_2NNH_2) were purchased from Alfa Aesar. NMR spectra were recorded on a Mercury Plus-400 spectrometer. Elemental analyses were performed with an Elementar VarioEL III instrument. IR spectra were recorded using a Nicolet AVATAR 360 FT-IR spectrometer.

Ring open polymerization (ROP) of cyclic esters – General procedure

In the glovebox, a Schlenk tube was charged with the stock solutions of the catalyst and with the required amount of a toluene solution of benzyl alcohol. The mixture was stirred for 2 min at room temperature and then the monomer (2.5 mmol) along with 1.5 mL toluene were added. The reaction mixture was then placed into an oil bath pre-heated to the required temperature, and the solution was stirred for the required time. The polymerization mixture was then quenched by addition of an excess of glacial acetic acid (0.2 mL); the solution was then poured into methanol (200 mL) and the resultant polymer was then collected on filter paper and dried *in vacuo*.

Kinetic studies

The polymerizations were carried out at 80 °C in a glovebox. The monomer to initiator ratio was fixed at 500:1. At appropriate time intervals, 0.5 mL aliquots were removed (under N_2) and were quenched with wet $CDCl_3$. The percent conversion was determined by ^{1}H NMR spectroscopy.

***Synthesis of* [O=C(Me)C(Me)=NAr] (Ar = 2,6-*i*Pr$_2$C$_6$H$_3$ and 2,6-Et$_2$C$_6$H$_3$) (L$^{i\text{Pr-NO}}$ and L$^{\text{Et-NO}}$)**

To a stirred solution of diacetyl (2,3-butanedione) (0.12 mol, 10.5 mL) in *n*-hexane (80.0 mL), 2,6-diisopropylaniline (0.10 mol, 18.9 mL) or 2,6-diethylaniline (0.10 mol, 16.5 mL) was added drop-wise in the presence of the catalytic amount of formic acid. The solution was stirred for 24 h at room temperature. The reaction progress was checked by TLC. The products were isolated as yellow liquids by vacuum distillation (**L$^{i\text{pr-NO}}$** 140 ºC/0.3 mmHg, 19.60 g, 80%; **L$^{\text{Et-NO}}$** 104 ºC/0.3 mmHg, 16.60 g, 78%). **L$^{i\text{Pr-NO}}$**: ^{1}H NMR (400 MHz, $CDCl_3$): δ = 1.13 (d, J = 5.2 Hz, 6H; CH(CH_3)$_2$), 1.14 (d, J = 5.2 Hz, 6H; CH(CH_3)$_2$), 1.82 (s, 3H CCH_3), 2.56 (m, 2H; CH(CH$_3$)$_2$), 2.58 (s, 3H CCH_3), 7.09−7.17 (m, 3H; Ar). ^{13}C NMR (100.6 MHz, $CDCl_3$): δ = 15.0 (N−CCH$_3$), 22.7 (CH(CH_3)$_2$), 23.2 (CH(CH_3)$_2$), 25.0 (O=C CH_3), 28.4 (CH(CH$_3$)$_2$), 123.1, 124.5, 128.3, 129.1, 134.6, 145.1 (Ar), 166.8 (N=CCH$_3$), 200.0 ppm (O=CCH$_3$). IR (Nujol, cm^{-1}): ν = 3384w, 3082 m, 2967 s, 2881 s, 1918 w, 1852 w, 1714 s, 1642 s, 1584 w, 1455 s, 1340 s, 1325 m, 1282 w, 1253 m, 1196 m, 1123 s, 1051 m, 994 w, 921 m, 821 m, 763 s, 735 m, 677 w, 604 w, 518 w, 446 w.

L$^{Et\text{-}NO}$: ^{1}H NMR (400 MHz, DMSO-d_6): δ = 1.04 (t, J = 7.6 Hz, 6H; CH_2CH_3), 1.70 (s, 3H CCH_3), 2.24 (q, 4H; CH_2CH_3), 2.48 (s, 3H CCH_3), 6.99−7.10 (m, 3H; Ar). ^{13}C NMR (100.6 MHz, $CDCl_3$): δ = 13.6 (N=CCH_3), 14.7 (CH_2CH_3), 24.8 (CH_2CH_3), 124.2, 126.2, 128.2, 129.0, 130.0, 146.4 (Ar), 166.5 (N=CCH_3), 200.0 ppm (O=CCH_3). IR (Nujol, cm^{-1}): ν = 3384w, 3079 m, 2957 s, 2881 s, 1919 w, 1858 w, 1690 s, 1644 s, 1582 w, 1445 s, 1339 s, 1308 m, 1201 m, 1109 s, 1048 w, 987 w, 942 w, 865 m, 834 s, 758 s, 605 w, 529 m.

***Synthesis of* [ArN=C(Me)C(Me)=N-]$_2$ (Ar = 2,6-*i*Pr$_2$C$_6$H$_3$) (L$^{ipr\text{-}N_4}$)**

To a solution of 3-(2,6-diisopropylphenylimino)butan-2-one (**L$^{ipr\text{-}NO}$** 0.05 mol, 12.3 mL) in ethanol (50 mL), a solution of hydrazine (0.030 mol, 1.0 mL) in ethanol (5 mL) was added in the presence of the catalytic amount of formic acid. The mixture was stirred for 24 h at room temperature affording the title compound as a yellow formed that was isolated by filtration, washed with ethanol (2×10 ml) and dried in vacuum. Yield 75%. ^{1}H NMR (400 MHz, $CDCl_3$): δ = 1.18 (d, J = 2.4 Hz, 24H; $CH(CH_3)_2$),2.05 (s, 6H CCH_3), 2.26 (s, 6H; CCH_3), 2.68 (sept, 4H; $CH(CH_3)_2$), 7.07−7.20 (m, 6H; Ar). ^{13}C NMR (100.6 MHz, $CDCl_3$): δ = 13.1 (CCH_3), 16.5 (CCH)), 22.9 ($CH(CH_3)_2$), 23.3 ($CH(CH_3)_2$), 28.5 ($CH(CH_3)_2$), 123.1, 124.0, 135.4, 146.1 (Ar), 156.9 (N=CCH_3), 166.2 ppm (N=CCH_3). IR (Nujol, cm^{-1}): ν = 3415 w, 3247 w, 2866 m, 2347 w, 1934 w, 1842 w, 1629 s, 1598 s, *1582 w, 1476 s, 1369 s, 1308 m, 1247 m, 1201 s, 1109 s, 926 w, 834 w, 758 s, 697 m, 636 w, 453 w.*

***Synthesis of* {[ArNC(Me$_2$)C(Me)=NAr]AlMe$_2$} (Ar = 2,6-iPr$_2$C$_6$H$_3$, 1)**

AlMe3 (3.0 mmol, 0.216 g) was added to a solution of LiPr (3.0 mmol, 1.214 g) in 30 mL of toluene, and the mixture was stirred at room temperature for 12 h. The solution was then filtered and concentrated to about 5 mL. Yellow crystals were obtained upon standing at −20 °C (1.170 g, 82%). ^{1}H NMR (400 MHz, $CDCl_3$): δ = –0.93 (s, 6H; $Al(CH_3)_2$), 1.03 (d, J = 4.4 Hz, 6H; $CH(CH_3)_2$), 1.07 (d, J = 4.4 Hz, 6H; $CH(CH_3)_2$), 1.21 (d, J = 4.4 Hz, 6H; $CH(CH_3)_2$), 1.24 (d, J = 4.4 Hz, 6H; $CH(CH_3)_2$), 1.27 (s, 6H N–$C(CH_3)_2$), 1.95 (s, 3H

N=CCH_3), 2.97 (sept, J = 4.4 Hz, 2H; CH(CH_3)$_2$), 3.67 (sept, J = 4.4 Hz, 2H; CH(CH_3)$_2$), 7.04−7.29 (m, 6H ; Ar). ^{13}C NMR (100.6 MHz, $CDCl_3$): δ = –7.5 (Al(CH_3)$_2$), 18.6 (N=CCH_3), 24.0 (N–C(CH_3)$_2$), 24.3 (CH(CH_3)$_2$), 24.9 (CH(CH_3)$_2$), 27.6 (CH(CH_3)$_2$), 27.8 (CH(CH_3)$_2$), 27.9 (CH(CH_3)$_2$), 28.2 (CH(CH_3)$_2$), 67.5 (N–C(CH_3)$_2$), 123.4, 124.0, 124.7, 127.9, 138.1, 141.2, 142.6, 151.3 (Ar), 198.6 ppm (N=$C$$CH_3$). IR (Nujol, cm^{-1}): ν = 3415 w, 2895 s, 2697 w, 2361 w, 1629 m, 1445 s, 1353 s, 1232 m, 1171 m, 1124 m, 1063 m, 865 m, 789 m, 727 s, 636 m, 468 w. Elemental analysis calcd. for $C_{31}H_{49}AlN_2$ (476.70): C 78.10; H 10.36; N 5.88. Found: C 77.70, H 10.95 N 5.89%.

***Synthesis of* {[ArNC(Me$_2$)C(Me)=NAr]AlMe$_2$} (Ar = 2,6-Et$_2$C$_6$H$_3$, 2).**

Following the procedure described for **1**, complex **2** was prepared by reacting $AlMe_3$ (3.0 mmol, 0.216 g) with **L^{Et}** (3.0 mmol, 1.046) in 30 mL of toluene. Yellow crystals (1.002 g, 79%); ^{1}H NMR (400 MHz, $CDCl_3$): δ = –0.95 (s, 6H; Al(CH_3)$_2$), 1.18 (t, J = 7.6 Hz, 6H; CH_2CH_3), 1.24 (t, J = 7.6 Hz, 6H; CH_2CH_3), 1.30 (s, 6H; N–C(CH_3)$_2$), 1.93 (s, 3H; N=CCH_3), 2.45 (m, 2H CH_2CH$_3$), 2.65 (m, 4H CH_2CH$_3$), 3.08 (m, 2H CH_2CH$_3$), 7.05−7.29 (m, 6H ; Ar). ^{13}C NMR (100.6 MHz, $CDCl_3$): δ = –7.8 (Al(CH_3)$_2$), 14.1 (CH_2CH_3), 16.0 (CH_2CH_3), 17.7 (N=CCH_3) 23.4 (CH_2CH_3), 25.0 (CH_2CH_3), 27.3 (N–C(CH_3)$_2$), 68.9 (N–C(CH_3)$_2$), 123.5, 125.7, 126.6, 127.3, 135.6, 139.7, 144.3, 146.6 (Ar), 197.8 ppm (N=$C$$CH_3$). IR (Nujol, cm^{-1}): 2926 s, 1659 s, 1582 w, 1445 w, 1369 m, 1247 w, 1124 m, 1018 w, 727m, 682 w, 484 w. Elemental analysis calcd. for $C_{27}H_{41}AlN_2$ (420.60): C 77.10; H 9.83; N 6.66. Found: C 76.88, H 10.25 N 6.43%.

***Synthesis of* {[ArNC(Me$_2$)C(Me)=NAr]AlMe$_2$} (Ar = 2,6-Me$_2$C$_6$H$_3$, 3).**

Following the procedure described for **1**, complex **3** was prepared by reacting $AlMe_3$ (3.0 mmo, 0.220 g) with **L^{Me}** (3.0 mmol, 0.900 g) to afford yellow crystals (0.880 g, 80%). ^{1}H NMR (400 MHz, $CDCl_3$): δ = –0.78 (s, 6H; Al(CH_3)$_2$), 1.49 (s, 6H; N–C(CH_3)$_2$), 2.03 (s, 3H; N=CCH_3), 2.31 (s, 6H; Ar-CH_3), 2.50 (s, 6H; Ar-CH_3), 7.04−7.26 (m, 6H ; Ar). ^{13}C NMR (100.6 MHz, $CDCl_3$): δ = –7.1 (Al(CH_3)$_2$), 17.1 (N=CCH_3), 18.0 (N–C(CH_3)$_2$), 21.0 (Ar-CH_3), 27.4 (Ar-CH_3), 69.6 (N–C(CH_3)$_2$), 123.1, 126.9, 128.3, 129.2, 129.9, 140.9, 141.0, 146.1 (Ar), 197.5 ppm (N=$C$$CH_3$). IR (Nujol, cm^{-1}): 2911 s, 1934 w, 1858 w,

1622 s, 1461 s, 1369 s, 1216 s, 1171 s, 1140 s, 1109 m, 1018 m, 880 m, 789 s, 713 s, 651 s, 590 s, 484 m, 622 m. Elemental analysis calcd. for $C_{23}H_{33}AlN_2$ (364.49): C 75.79; H 9.13; N 7.69. Found: C 75.78, H 9.64 N 7.55%.

***Synthesis of* [ArN–C(Me)$_2$C(Me)=NAlMe$_2$]$_2$ (Ar = 2,6-*i*Pr$_2$C$_6$H$_3$, 4).**

$AlMe_3$ (6.0 mmol, 0.432 g) was added to a solution of $\mathbf{L}^{i\mathbf{Pr\text{-}N4}}$ (3.0 mmol, 1.460 g) in 30 mL of toluene, and the mixture was stirred at room temperature for 12 h. A color changed (from yellow to green) was observed. The mixture was filtered and concentrated to about 5 mL. Light-green crystals were obtained upon standing at −20 °C (1.358 g, 72%). ^{1}H NMR (400 MHz, $CDCl_3$): δ = –0.87 (s, 6H; Al(CH_3)$_2$), –0.81 (s, 6H; Al(CH_3)$_2$), 1.01 (d, J = 6.8 Hz, 6H; CH(CH_3)$_2$), 1.06 (d, J = 6.8 Hz, 6H; CH(CH_3)$_2$), 1.20 (s, 6H N–C(CH_3)$_2$), 1.21 (d, J = 6.8 Hz, 6H; CH(CH_3)$_2$), 1.22 (d, J = 6.8 Hz, 6H; CH(CH_3)$_2$), 1.56 (s, 6H N–C(CH_3)$_2$), 1.96 (s, 3H N=CCH_3), 2.24 (s, 3H N=CCH_3), 2.81 (sept, J = 6.8 Hz, 2H; CH(CH$_3$)$_2$), 3.60 (sept, J = 6.8 Hz, 2H; CH(CH$_3$)$_2$), 6.92−7.29 (m, 6H ; Ar). ^{13}C NMR (100.6 MHz, $CDCl_3$): δ = –7.4 (Al(*C*H$_3$)$_2$), –5.5 (Al(*C*H$_3$)$_2$), 17.2 (N=C*C*H$_3$), 18.4 (N=C*C*H$_3$), 24.0 (N–C(*C*H$_3$)$_2$), 24.3 (N–C(*C*H$_3$)$_2$), 25.0 (CH(*C*H$_3$)$_2$), 26.3 (CH(*C*H$_3$)$_2$), 27.3 (CH(*C*H$_3$)$_2$), 27.7 (CH(*C*H$_3$)$_2$), 27.8 (*C*H(CH$_3$)$_2$), 28.2 (*C*H(CH$_3$)$_2$), 65.1 (N–*C*(CH$_3$)$_2$), 66.8 (N–*C*(CH$_3$)$_2$), 123.2, 123.5, 125.0, 128.4, 137.0, 141.1, 143.8, 151.3 (Ar), 191.2, 196.5 ppm (N=*C*CH$_3$). IR (Nujol, cm^{-1}): 2911 s, 2866 s, 1613 m, 1552 m, 1461 s, 1369 s, 1201 m, 1140 s, 942 m, 789 w, 743 m, 682 m, 590 w, 484 w. Elemental analysis calcd. for $C_{38}H_{64}Al_2N_4$ (630.89): C 72.34; H 10.22; N 8.88. Found: C 72.43, H 10.65, N 8.66%.

***Synthesis of* {[OCMe$_2$CH(Me)=NAr]AlMe$_2$}$_2$ (Ar = 2,6-Et$_2$C$_6$H$_3$, 5).**

$AlMe_3$ (3.0 mmol, 0.216 g) was added to a solution of $\mathbf{L}^{\mathbf{Et\text{-}NO}}$ (3.0 mmol, 0.652 g) in 30 mL of toluene, and the mixture was stirred at room temperature for 12 h. A color change (from yellow to pale yellow) was observed. The reaction mixture was filtered and concentrated to about 5 mL. Colourless crystals of **5** were obtained upon standing at −20 °C (0.667 g, 77%). ^{1}H NMR (400 MHz, THF-d_8): δ = –0.92 (s, 12H; Al(CH_3)$_2$), 1.16 (t, J = 4.8 Hz, 12H; CH$_2$CH_3), 1.59 (s, 12H; N–C(CH_3)$_2$), 1.76 (s, 6H; N=C*C*H$_3$), 2.31 (m, 4H CH_2CH$_3$), 2.55 (m, 4H CH_2CH$_3$), 7.10−7.18 (m, 6H; Ar). ^{13}C NMR (100.6 MHz,

THF-d_8): δ = –3.3 (Al(CH_3)$_2$), 14.7 (CH_2CH_3), 17.0 (CH_2CH_3), 24.5 (N=CCH_3), 27.8 (O–C(CH_3)$_2$), 78.0 (O–C(CH_3)$_2$), 126.5, 126.9, 135.7 (Ar), 144.1 ppm (N=$C$$CH_3$). IR (Nujol, cm^{-1}): 2926 s, 2835 s, 1644 s, 1582 m, 1461 s, 1384 s, 1155 m, 1124 m, 972 m, 880 m, 773 m, 743 s, 666 s, 544 w, 468 w. Elemental analysis calcd. for $C_{34}H_{56}Al_2N_2O_2$ (578.76): C 70.56; H 9.75; N 4.84. Found: C70.29, H 10.13, N 4.83%.

***Synthesis of* {[ArNC(Me)(Et)C(Me)=NAr]ZnEt} (Ar = 2,6-*i*Pr$_2$C$_6$H$_3$, 6)**

$ZnEt_2$ (3.0 mmol, 0.371 g) was added to a solution of **L^{iPr}** (3.0 mmol, 1.214 g) in 30 mL of toluene, and the mixture was stirred at room temperature for 12 h. A color change (from yellow to pale yellow) was observed. The reaction mixture was filtered and concentrated to about 5 mL. Light-yellow crystals of **6** were obtained upon standing at −20 °C (1.230 g, 78%). ^{1}H NMR (400 MHz, $CDCl_3$): δ = –0.15 (q, J = 5.6 Hz, 2H; Zn–CH_2CH$_3$), 0.88 (t, J = 5.6 Hz, 3H; Zn–CH$_2$CH_3), 1.03–1.07 (m, 9H; C–CH$_2$CH_3 and CH(CH_3)$_2$), 1.21 (s, 3H; N–CCH_3(Et)), 1.24–1.34 (m, 18H, CH(CH_3)$_2$), 1.63 (sept, 1H, CH(CH$_3$)$_2$), 1.74 (sept, 1H, CH(CH$_3$)$_2$), 1.90 (s, 3H, N=CCH_3), 2.91 (m, 2H; C–CH_2CH$_3$), 3.76 (sept, 2H, CH(CH$_3$)$_2$), 7.09–7.27 (m, 6H ; Ar). ^{13}C NMR (100.6 MHz, C_6D_6): δ = –2.1 (Al–CH$_2$CH$_3$), 9.1 (Al–CH$_2$$CH_3$), 12.1 (C–CH$_2$$CH_3$), 17.9 (N=C$CH_3$), 22.2 (N–C$CH_3$(Et)), 22.6 (C–C$H_2CH_3$), 23.4 (CH($CH_3$)$_2$), 23.9 (CH($CH_3$)$_2$), 24.1 (CH($CH_3$)$_2$), 24.4 (CH($CH_3$)$_2$), 25.4 (CH($CH_3$)$_2$), 26.3 (CH($CH_3$)$_2$), 26.5 (CH($CH_3$)$_2$), 27.0 (CH($CH_3$)$_2$), 28.5 ($C$H(CH$_3$)$_2$), 28.6 ($C$H(CH$_3$)$_2$), 28.8 ($C$H(CH$_3$)$_2$), 32.7 ($C$H(CH$_3$)$_2$), 70.7 (N–$C$Me(Et)), 122.4, 122.9, 123.8, 126.0, 138.4, 142.6, 147.5, 149.7, 150.4 (Ar), 190.8 (N=CCH$_3$). IR (Nujol, cm^{-1}): 2926 s, 2697 w, 1629 m, 1445 s, 1384 s, 1292 w, 1216 w, 1140 w, 1032 w, 926 w, 789 m, 713 s, 697 m, 590 w, 529 w, 453 m. Elemental analysis calcd. for $C_{32}H_{50}ZnN_2$ (528.11): C 72.77; H 9.54; N 5.30. Found: C 72.35, H 9.86, N 5.20%.

***Synthesis of* {[ArN=C(Me)COCHCO(Me)C(Me)=NAr][OCH(Me)C(Me)=NAr](ZnEt)$_3$} (Ar = 2,6-*i*Pr$_2$C$_6$H$_3$, 7)**

$ZnEt_2$ (3.0 mmol, 0.371 g) was added to a solution of **L$^{iPr\text{-}NO}$** (3.0 mmol, 0.736 g) in 30 mL of toluene, and the mixture was stirred at r.t. for 12 h. A color changed (from yellow to pale yellow) was observed. The reaction mixture was filtered and concentrated to about

5 mL. Colourless crystals of **7** were obtained upon standing at −20 °C (1.426 g, 47%). ^{1}H NMR (400 MHz, $CDCl_3$): δ = –0.01 (q, J = 5.6 Hz, 6H; Zn–CH_2CH$_3$), 1.04–1.06 (d, 9H; CH(CH_3)$_2$), 1.11–1.14 (t, J = 5.6 Hz,9H; Zn–CH$_2$CH_3), 1.14–1.15 (m, 6H; O–CCH_3 and O–CHCH_3), 1.25–1.30 (m, 27H, CH(CH_3)$_2$), 1.74 (s, 9H, N=CCH_3), 2.83 (sept, 3H, CH(CH$_3$)$_2$), 3.09 (sept, 3H, CH(CH$_3$)$_2$), 4.69 (m, 2H, C=CH and O-CH-C=N), 7.15–7.23 (m, 9H, Ar). ^{13}C NMR (100.6 MHz, $CDCl_3$): δ = –3.58 (Zn–CH$_2$CH$_3$), 13.1 (N=CCH$_3$), 18.5 (Zn–CH$_2$CH$_3$), 23.7 (CH(CH$_3$)$_2$), 24.2 (CH(CH$_3$)$_2$), 24.5 (CH(CH$_3$)$_2$), 24.7 (CH(CH$_3$)$_2$), 25.7 (CH(CH$_3$)$_2$), 23.6 (CH(CH$_3$)$_2$), 23.7 (CH(CH$_3$)$_2$), 24.2 (CH(CH$_3$)$_2$), 24.5 (CH(CH$_3$)$_2$), 25.4 (CH(CH$_3$)$_2$), 27.5 (CH(CH$_3$)$_2$), 27.7 (CH(CH$_3$)$_2$), 71.1 (O–C), 123.6, 124.2, 125.8, 139.0, 140.3, 142.1 (Ar and C=C), 190.0 (N=CCH$_3$). IR (Nujol, cm^{-1}): 2926 s, 2713 w, 1644 m, 1445 s, 1369 s, 1186 w, 1124 m, 1018 m, 956 m, 911 m, 850 w, 789 m, 727 s, 590 m, 498 m. Elemental analysis calcd. for $C_{54}H_{83}Zn_3N_3O_3$•0.5toluenen (1018.34): C 64.88; H 8.24; N 3.95. Found: C 64.40, H 8.70, N 4.01%.

Synthesis of $\mathbf{L^{iPr\text{-}N_2\text{-}ArCH_2Ar\text{-}N_2}}$

To a solution of 3-(2,6-diisopropylphenylimino)butan-2-one ($\mathbf{L}^{ipr\text{-}NO}$ 0.025 mol, 6.2 mL) in methanol (30 mL), a solution of 4,4′-methylenebis-(2,6-diisopropylaniline) (0.010 mol, 3.7 g) in toluene (5 mL) was added drop-wise in the presence of the catalytic amount of formic acid. The mixture was stirred for 48 h at room temperature affording a yellow precipitate which was isolated by filtration, washed with 2×10 ml ice methanol, and dried in vacuum to afford the title compound as a yellow powder in 80% yield (6.6 g). ^{1}H NMR (400 MHz, $CDCl_3$): δ = 1.15-1.20 (d, J = 6.8 Hz, 48H, CH(CH_3)$_2$), 2.07 (s, 6H, N=CCH_3),2.09 (s, 6H, N=CCH_3), 2.70 (sept, J = 6.8 Hz, 4H; CH(CH$_3$)$_2$), 2.71 (sept, J = 6.8 Hz, 4H; CH(CH$_3$)$_2$), 4.03 (s, 2H, (C$_6$H$_2$)$_2$CH_2), 7.00 (s, 4H, (C$_6H_2$)$_2$CH$_2$), 7.10 (t, J = 7.5 Hz, 2H, p-C$_6$H$_3$), 7.17 (d, J = 7.5 Hz, 4H，m-C$_6$H$_3$). ^{13}C NMR (100.6 MHz, $CDCl_3$): δ = 16.7 (N=CCH$_3$), 16.8 (N=CCH$_3$), 22.8 (CH(CH$_3$)$_2$), 23.0 (CH(CH$_3$)$_2$), 23.2 (CH(CH$_3$)$_2$), 23.2 (CH(CH$_3$)$_2$), 28.7 (CH(CH$_3$)$_2$) 41.6 ((C$_6$H$_2$)$_2C$H$_2$), 123.1 (p-C$_6$H$_2$), 123.8 (p-C$_6$H$_3$), 135.2 (m-C$_6$H$_2$), 135.2 (m-C$_6$H$_3$) 136.6 (o-C$_6$H$_2$), 144.2 (NC$_6$H$_2$), 146.4 (NC$_6$H$_3$), 168.4 (N=CCH$_3$), 168.6 (N=CCH$_3$). IR (Nujol, cm^{-1}): 2962 s, 2928 s , 2900 s, 2870 s, 1651 s, 1468 s, 1436 s, 1384 m, 1362 s, 1329 w, 1297 w,1252 w, 1193 m, 1165 w, 1120 s, 954

w,937 m, 882 w, 850 m, 803 m, 780 m, 759 s, 689 m, 467 w, 430 w. Elemental analysis calcd. For $C_{57}H_{80}N_4$ (821.25): C, 83.36; H, 9.82; N, 6.82; Found: C 83.47, H 9.39, N 6.70%. M.P = 168-170 ºC.

Synthesis of **[$L^{iPr\text{-}N_2\text{-}ArCH_2Ar\text{-}N_2}(ZnCl_2)_2$] (8)**

$ZnCl_2$ (6.0 mmol, 0.816 g) was added to a solution of $L^{iPr\text{-}N_2\text{-}ArCH_2Ar\text{-}N_2}$ (3.0 mmol, 2.463 g) in 30 mL of CH_2Cl_2, and the mixture was stirred at reflux for 12 h. The reaction mixture was filtered and concentrated to about 5 mL. Yellow crystals were obtained upon standing at −20 °C, washed with 2×5 ml cold toluene, and dried in vacuum to afford a yellow powder (2.560 g, 78%). ^{1}H NMR (400 MHz, $CDCl_3$): δ = 1.12-1.14 (d, J = 6.8 Hz, 24H, CH(CH_3)$_2$), 1.34-1.36 (d, J = 6.8 Hz, 24H, CH(CH_3)$_2$), 2.36 (s, 6H, N=CCH_3), 2.39 (s, 6H, N=CCH_3), 2.93 (sept, J = 6.8 Hz, 8H; CH(CH$_3$)$_2$), 3.98 (s, 2H, (C$_6$H$_2$)$_2$CH_2), 7.18 (s, 4H，(C$_6H_2$)$_2$CH$_2$). 7.25 (t, J = 7.5 Hz, 2H, p-C$_6$H$_3$), 7.28 (d, J = 7.5 Hz, 4H, m-C$_6$H$_3$). ^{13}C NMR (100.6 MHz, $CDCl_3$): δ = 20.4 (N=CCH$_3$), 20.5 (N=CCH$_3$), 21.6 (CH(*C*H$_3$)$_2$), 24.5 (CH(*C*H$_3$)$_2$), 24.7 (CH(*C*H$_3$)$_2$), 24.8 (CH(*C*H$_3$)$_2$), 29.0 (*C*H(CH$_3$)$_2$) 42.0 ((C$_6$H$_2$)$_2$*C*H$_2$), 124.8 (p-C$_6$H$_2$), 125.4 (p-C$_6$H$_3$), 128.4 (m-C$_6$H$_2$), 129.2 (m-C$_6$H$_3$) 138.0 (o-C$_6$H$_2$), 139.2 (NC$_6$H$_2$), 139.5 (NC$_6$H$_3$), 169.6 (N=*C*CH$_3$), 169.8 (N=*C*CH$_3$). IR (Nujol, cm^{-1}): 2967 s, 2927 s, 2866 s, 1637 s, 1466 s, 1444 s, 1370 s, 1365 s,1326 m,1307 w, 1249 w, 1216 s, 1188 m, 1147 m, 1122 m, 853 m, 833 m, 793 m, 764 w, 739 w 465 w. Elemental analysis calcd. For $C_{57}H_{80}Cl_4N_4Zn_2$·2toluene (1272.50): C, 66.72; H, 7.57; N, 4.38; Found: C 66.43, H 7.40, N 4.72%.

X-ray Crystallographic Analysis

Diffraction data for complexes $L^{iPr\text{-}N_4}$, $L^{iPr\text{-}N2\text{-}ArCH2Ar\text{-}N2}$, **1**–**8** were collected on a Bruker SMART APEX II diffractometer at 153 K with graphite-monochromated Mo Kα radiation (λ = 0.71073 Å). An empirical absorption correction using SADABS was applied for all data. [28] The structures were solved and refined to convergence on F^2 for all independent reflections by the full-matrix least squares method using the SHELXL−2014 programs. [29] In compound **7**, about 2 molecules of toluene (about 0.5 toluene molecules per formula, Z = 4) are co-crystallized, with the corresponding electron density (98 electrons).

View Article Online
DOI: 10.1039/C9DT04332B

In compound **8**, about 14 molecules of toluene (about 3.5 toluene molecules per formula, Z = 4) are co-crystallized, with the corresponding electron density (564 electrons). Crystallographic data and refinement details for compounds $\mathbf{L}^{i\mathbf{Pr}\text{-}\mathbf{N_4}}$, $\mathbf{L}^{\mathbf{iPr}\text{-}\mathbf{N_2}\text{-}\mathbf{ArCH_2Ar}\text{-}\mathbf{N_2}}$, **1–8** are given in Tables S1–S3. CCDC numbers 1957505–1957511 for compounds $\mathbf{L}^{\mathbf{iPr}\text{-}\mathbf{N_4}}$, **2**–**3** and **4**–**7**, CCDC numbers 1961896 and 1961898 for compounds $\mathbf{L}^{\mathbf{iPr}\text{-}\mathbf{N_2}\text{-}\mathbf{ArCH_2Ar}\text{-}\mathbf{N_2}}$ and **8**. These data can be obtained free of charge from the Cambridge Crystallographic Data Centre www.ccdc.cam.ac.uk/data_request/cif.

Conflicts of interest

There are no conflicts of interest to declare.

Acknowledgments

We thank the Shaanxi Provincial Department of Education Key Laboratory Project (19JS065) and China Postdoctoral Science Foundation (2016M602849) for financial support. CR thanks the Shaanxi Province for the 100 talents award, Northwest University for financial support and the EPSRC for an Overseas travel grant (EP/R023816/1) and the Evolving a circular economy grant (EP/S025537/1). The National Mass Spectrometry Centre at Swansea is thanked for data.

References

[1] For reviews, see (a) B. J. O'Keefe, M. A. Hillmeyer and W. B. Tolman, *J. Chem. Soc., Dalton Trans*., 2001, 2215-2224; O. Dechy-Cabaret, B. Martin-Vaca and D. Bourissou, *Chem. Rev*., 2004, **104**, 6147–6176; (b) M. Labet and W. Thielemans, *Chem. Soc. Rev*., 2009, **38**, 3484–3504; (c) C. M. Thomas, *Chem. Soc. Rev*., 2010, **39**, 165–173; (d) A. Arbaoui and C. Redshaw, *Polym. Chem*., 2010, **1**, 801– 826; (e) Y. Sarazin, J.-F. Carpentier, *Chem. Rev*. 2015, **115**, 3564−3614 and references therein.

[2] (a) J. Wu, T.-L. Yu, T. Chen and C.-C. Lin, *Coord. Chem. Rev*. 2006, **250**, 602–626; (b) Y. Wei, S. Wang and S. Zhou, *Dalton Trans*. 2016, **45**, 4471–4485; (c) J. Gao, D. Zhu, W. Zhang, G. A. Solan, Y. Ma and W. –H. Sun, *Inorg. Chem. Frontiers* 2019, **6**, 2619–2652.

[3] (a) S. D. Ittel, L. K. Johnson and M. Brookhart, *Chem. Rev.* 2000, **100**, 1169–1204; (b)

Recent Progress in Late Transition Metal α-Diimine Catalysts for Olefin Polymerization. Zhibin Guan and Chris S. Popeney, Part of the *Topics in Organometallic Chemistry* book series Springer 2008; (c) R. Gao, W. -H. Sun and C. Redshaw, *Cat. Sci & Tech*. 2013, **3**, 1172–1179; (d) S. Wang, W. -H. Sun and C. Redshaw, *J. Organomet. Chem.* 2014, **751**, 717–741; (e) F. Wang and C. Chen, *Polym. Chem*. 2019, **10**, 2354-2369.

[4] (a) J. M. Klerks, D. J. Stufkens, G. van Koten and K. Vrieze, *J. Organomet. Chem*. 1979, **181**, 271–283; (b) V. C. Gibson, C. Redshaw, A. J. P. White and D. J. Williams, *J. Organomet Chem.* 1998, **550**, 453–456; (c) M. Bruce, V. C. Gibson, C. Redshaw, G. A. Solan, A. J. P. White and D. J. Williams, *Chem. Commun*. 1998, 2523–2524; (d) V. C. Gibson, D. Nienhuis, C. Redshaw, A. J. P. White and D. J. Williams, *Dalton Trans.* 2004, 1761–1765; (e) V. C. Gibson, C. Redshaw, G. A. Solan, A. J. P. White and D. J. Williams, *Organometallics* 2007, **26**, 5119–5123; (f) A. Arbaoui, C. Redshaw and D. L. Hughes, *Chem. Comm*. 2008, 4717–4719; (g) A. Arbaoui, C. Redshaw and D. L. Hughes. *Supramol Chem*. 2009, **21**, 35–43; (h) J. A. Olson, R. Boyd, J. W. Quail, S. R. Foley, *Organometallics* 2008, **27**, 5333–5338.

[5] (a) M. Delferro and T. J. Marks, T. J. *Chem. Rev*. 2011, **111**, 2450–2485; (b) H.-C. Tseng, H. Y. Chen, Y. –T. Huang, W. –Y. Lu, Y. –L. Chang, M. Y. Chiang, Y. –C. Lai, H. –Y. Chen, *Inorg. Chem*. 2016, **55**, 1642-1650; (c) C. Redshaw, *Catalysts*, 2017, **7**, 165.

[6] (a) H. -K. Luo and H. Schumann, *J. Mol. Cat. A: Chem*. 2005, **227**, 153–161; (b) S. Jie, D. Zhang, T. Zhang, W. -H. Sun, J. Chen, Q. Ren, D. Liu, G. Zheng and W. Chen, *J. Organomet. Chem*. 2005, **690**, 1739–1749; (c) J. D. A. Pelletier, J. Fawcett, K. Singh and G. A. Solan, *J. Organomet. Chem*. 2008, **693**, 2723–2731; (d) S. Kong, K. Song, T. Liang, C. -Y. Guo, W. -H. Sun and C. Redshaw, *Dalton Trans*. 2013, **42**, 9176–9187; (e) L. Zhu, Z. -S. Fu, H. -J. Pan, W. Feng, C. Chen and Z. -Q. Fan, *Dalton Trans*. 2014, **43**, 2900–2906; (f) Q. Xing, K. Song, T. Liang, Q. Liu, W. -H. Sun and C. Redshaw, *Dalton Trans*. 2014, **43**, 7830–7837.

[7] (a) B. M. Chamberlain, M. Cheng, D. R. Moore, T. M. Ovitt, E. B. Lobkovsky and G. W. Coates, *J. Am. Chem. Soc*. 2001, **123**, 3229–3238; (b) M. D. Hannant, M. Schormann and M. Bochmann, *Dalton Trans*. 2002, 4071-4073; (c) J. Börner, U. Flörke, K. Huber, A. Döring, D. Kuckling, and S. Herres-Pawlis, *Chem. Eur. J*. 2009, **15**, 2362–2376; (d) J.

Börner, U. Flörke, A. Döring, D. Kuckling, M. D. Jones and S. Herres-Pawlis, *Sustainability* 2009, **1**, 1226–1239; (e) J. Börner, U. Flörke, T. Glöge, T. Bannenberg, M. Tamm, M. D. Jones, A. Döring, D. Kuckling, S. Herres-Pawlis, *J. Mol. Catal. A: Chem*., 2010, **316**, 139–145; (f) X. Wang, X. Liu, and J. Huang, *Chimia* 2017, **71**, 773–776; (g) D. O. Meléndez, J. A. Castro-Osma, A. Lara-Sánchez, R. S. Rojas and A. Otero, *J. Polym. Sci., Part A, Polym. Chem*. 2017, **55**, 2397-2407.

[8] (a) Y. Zhao, Y. Liu, L. Yang, J. -G. Yu, S. Li, B. Wu, and X. –J. Yang, *Chem. Eur. J.* 2012, **18**, 6022–6030; (b) J. Yu, X. -J. Yang, Y. Liu, Z. Pu, Q. -S. Li, Y. Xie, H. F. Schaefer and B. Wu, *Organometallics* 2008, **27**, 5800–5805; (c) Y. Liu, S. Li, X. -J. Yang, P. Yang, J. Gao, Y. Xia and B. Wu, *Organometallics* 2009, **28**, 5270–5272; (d) P. Yang, X. -J. Yang, J. Yu, Y. Liu, C. Zhang, Y. -H. Deng and B. Wu, *Dalton Trans.* 2009, 5773–5779; (e) Y. Liu, Y. Zhao, X. -J. Yang, S. Li, J. Gao, P. Yang, Y. Xia, and B. Wu, *Organometallics* 2011, **30**, 1599–1606; (f) I. L. Fedushkin, V. A. Dodonov, A. A. Skatova, V. G. Sokolov, A. V. Piskunov, G. K. Fukin, *Chem. Eur. J.* 2018, **24**, 1877–1889; (g) I. L. Fedushkin, A. N. Lukoyanov, S. Y. Ketkov, M. Hummert, H. Schumann, *Chem. Eur. J.* 2007, **13**, 7050–7056; (h) I. L. Fedushkin, A. A. Skatova, S. Y. Ketkov, O. V. Eremenko, A. V. Piskunov, G. K. Fukin, *Angew. Chem. Int. Ed.* 2007, **46**, 4302–4305; (i) I. L. Fedushkin, M. V. Moskalev, A. N. Lukoyanov, A. N. Tishkina, E. V. Baranov, G. A. Abakumov, *Chem. Eur. J.* 2012, **18**, 11264–11276; (j) O. V. Kazarina, C. Gourlaouen, L. Karmazin, A. G. Morozov, I. L. Fedushkin, S. Dagorne, *Dalton Trans.* 2018, **47**, 13800–13808.

[9] J. –M. Raquez, R. Mincheva, O. Coulembier, and P. Dubois, Ring-opening Polymerization of Cyclic Esters: Industrial Synthesis, Properties, Applications, and Perspectives. In Polymer Science: A Comprehensive Reference; Elsevier: Amsterdam, The Netherlands, 2012; pp. 761–777.

[10] (a) H. tom Dieck, M. Svoboda and T. Z. Grieser, *Naturforsch* 1981, **36b**, 823-832; (b) J. M. Kliegman, R. K. Bames, *J. Org. Chem*. 1970, **55**, 3140-3143; (c) R. van Asselt, Ph.D. Thesis, Universiteit van Amsterdam, 1993; (d) H. A. Zhong, J. A. Labinger and J. E. Bercaw, *J. Am. Chem. Soc.* 2002, **124**, 1378–1399.

[11] (a) L. Yang, D. R. Powell and R.P Houser, *Dalton Trans.* 2007, 955–964; A. W.

Addison, T. N. Rao, J. Reedijk, J. Van Rijn, G.C. Verschoor, *J. Chem. Soc., Dalton Trans.* 1984, 1349-1356.

[12] S. Milione, G. Cavallo, C. Tedesco and A. Grassi, *J. Chem. Soc*., *Dalton Trans*. 2002, 1839–1846

[13] E. Wissing, J. T. B. H. Jastrzebski, J. Boersma and G. Koten, *J. Organomet. Chem.* 1993, **459***,* 11–16.

[14] (a) H. Schumann, M. Hummert, A. N. Lukoyanov, I. L. Fedushkin, *Chem. Eur. J.* 2007, **13**, 4216–4222; (b) J. Scott, S. Gambarotta, I. Korobkov, Q. Knijnenburg, B. de Bruin, P. H. M. Budzelaar, *J. Am. Chem. Soc.* 2005, **127**, 17204–17206.

[15] (a) F. H. Van der Steen, G. P. M. Van Mier, A. L. Spek, J. Kroon, G. Van Koten, *J. Am. Chem. Soc.* 1991, **113**, 5742–5750; (b) Y.-L. Huang, B.-H. Huang, B.-T. Ko, C.-C. Lin, *J. Chem. Soc., Dalton Trans.* 2001, 1359–1365; (c) B.-H. Huang, T.-L. Yu, Y.-L. Huang, B.-T. Ko, C.-C. Lin, *Inorg. Chem.* 2002, **41,** 2987–2994; (d) M. Li, M. Chen, C. Chen, *Polymer* 2015, **64**, 234–239.

[16] (a) I. L. Fedushkin, A. N. Tishkina, G. K. Fukin, M. Hummert and H. Schumann, *Eur. J. Inorg. Chem.* 2008*, 4*83–489; (b) I. L. Fedushkin, V. M. Makarov, E. C. E. Rosenthal and G. K. Fukin, *Eur. J. Inorg. Chem*. 2006, 827–832; (c) A. N. Tishkina, A. N. Lukoyanov, A. G. Morozov, G. K. Fukin, K. A. Lyssenko and I. L. Fedushkin, *Russ. Chem. Bull.* 2009, **58**, 2250–2257.

[17] S. Schmidt, R. Schäper, S. Schulz, D. Bläser and C. Wölper, *Organometallics* 2011, **30**, 1073–1078.

[18] N. Hollingsworth, A. L Johnson, A. Kingsley, G. Kociok-Köhn and K. C. Molloy, *Organometallics* 2010, **29**, 3318–3326.

[19] J. A. Moore, K. Vasudevan, N. J. Hill, G. Reeske, A. H. Cowley, *Chem. Commun.* **2006**, 2913-2915.

[20] (a) Y. Zhao, Y. Liu, Y. Lei, B. Wu and X.-J. Yang, *Chem. Commun.* 2013, **49**, 4546–4548; (b) Y. Zhao, Y. Lei, Q. Dong, B. Wu and X. -J. Yang, *Chem. Eur. J.* 2013, **19**,

12059-12066; (c) W. Chen, Y. Zhao, W. Xu, J. -H. Su, L. Shen, L. Liu, B. Wu and X. -J. Yang, *Chem. Commun.* 2019, **55**, 9452–9455.

[21] *Biological Inorganic Chemistry: Structure and Reactivity*; H. B. Gray, E. I. Stiefel, J. S. Valentine, I. Bertini, Eds.; University Science Books: Sausalito, CA, 2006.

[22] (a) P. Buchwalter, J. Rosé, P. Braunstein, *Chem. Rev.* 2015, **115**, 28−126; (b) A. Velian, S. Lin, A. J. M. Miller, M. W. Day, T. Agapie, *J. Am. Chem. Soc.* 2010, **132,** 6296−6297.

[23] (a) T. Chu, G. I. Nikonov, *Chem. Rev.* 2018, **118**, 3608−3680; (b) Y.-Y. Zhou, C. Uyeda, *Science* 2019, **363**, 857–862.

[24] A. B. Kremer, R. J. Andrews, M. J. Milner, X. R. Zhang, T. Ebrahimi, B. O. Patrick, P. L. Diaconescu and P. Mehrkhodavandi, *Inorg. Chem*. 2017, **56,** 1375−1385.

[25] One reviewer has suggested the Al(II) species oxidatively adds the alcohol to initiate polymerization. On-going studies in our lab are investigating both the role played by the alcohol and the effects of steric and electronis on the ROP system of the Al-bounds ligands.

[26] (a) C. Ludwig and M. R. Viant, *Phytochem. Anal.* 2010, **21**, 22−32; (b) M. J. Walton, S. J. Lancaster and C. Redshaw, *ChemCatChem*, 2014, **6**, 1892−1898.

[27] (a) H. Hu, L. Zhang, H. Gao, F. Zhu and Q. Wu, *Chem. Eur. J.* 2014, **20**, 3225−3233; (b) G. Ricci, A. Sommazzi; G. Leone, A. Boglia and F. Masi, Patent WO2013037910 (A1)-2013-03-21; (c) M. Khoshsefat, G. H. Zohuri, N. Ramezanian, S. Ahmadjo and M. Haghpanah, *J. Polym. Sci., Part A: Polym. Chem*. 2016, **54**, 3000−3011.

[28] G. M. Sheldrick, Program SADABS: Area-Detector Absorption Correction, 1996, University of Göttingen, Germany.

[29] G. M. Sheldrick, *Acta Crystallogr., Sect. C: Cryst. Struct. Commun*., 2015, **71**, 3–8.

View Article Online
DOI: 10.1039/C9DT04332B

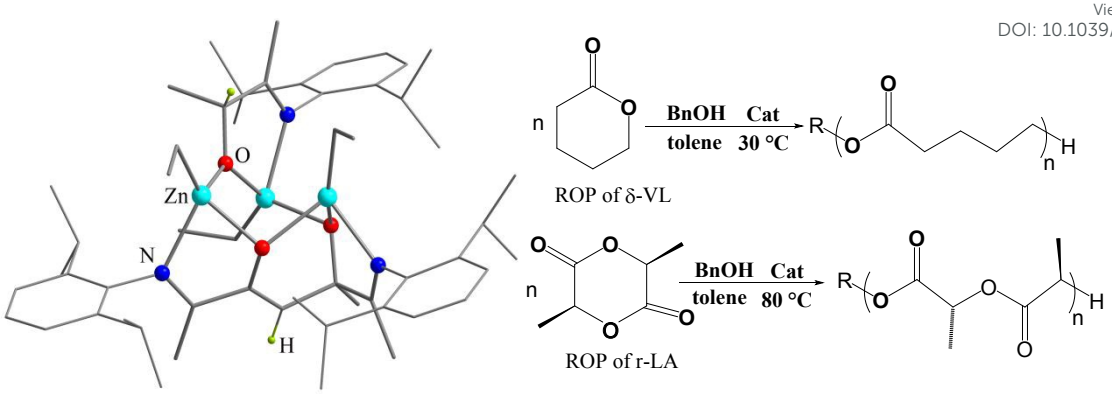

Multi-metallic complexes (of Al, Zn or Ga) derived from imine-based ligands can effectively operate as catalysts for the ring opening polymerization (ROP) of ε-caprolactone (ε-CL) and δ-valerolactone (δ-VL) and the co-polymerization thereof.